Polyampholytes

ANDREY V. DOBRYNIN,[1] RALPH H. COLBY,[2] MICHAEL RUBINSTEIN[3]

[1]Polymer Program, Institute of Materials Science and Department of Physics, University of Connecticut, Storrs, Connecticut 06269-3136

[2]Department of Materials Science and Engineering, Pennsylvania State University, University Park, Pennsylvania 16802

[3]Department of Chemistry, University of North Carolina, Chapel Hill, North Carolina 27599-3290

Received 26 November 2003; revised 17 February 2004; accepted 10 March 2004
DOI: 10.1002/polb.20207
Published online in Wiley InterScience (www.interscience.wiley.com).

ABSTRACT: Polyampholytes are charged polymers with both positively and negatively charged groups. The conformation of these polymers in solutions strongly depends on the distribution of charged monomers along the polymer backbone and their environment. In this review we summarize the current level of understanding of such amphoteric polymers in solutions and their interactions with surfaces and polyelectrolytes.
 J Polym Sci Part B: Polym Phys 42: 3513–3538, 2004
Keywords: polyampholytes; amphoteric polymers; interactions

INTRODUCTION

Polyampholytes are charged macromolecules carrying both acidic and basic groups.[1,2] Under appropriate conditions, such as in aqueous solutions, these groups dissociate, leaving ions on chains and counterions in solution. After ionization, there are positively and negatively charged groups on the polymer chain. Examples of polyampholytes include denatured proteins (e.g., gelatin), proteins in their native state (such as bovine serum albumin), and synthetic copolymers made of monomers with acidic and basic groups. If these groups are weak acids or bases, the net charge of a polyampholyte in aqueous solution can be changed by varying the pH. At a particular pH called the isoelectric point, there are equal numbers of positive and negative charges on the polyion, giving it a net charge of zero. In the vicinity of the isoelectric pH, the polymers are nearly charge-balanced and exhibit the unusual properties of polyampholytes. At high charge asymmetry (far above or far below the isoelectric pH), these polymers demonstrate polyelectrolyte-like behavior.[3–10]

In this review, we will describe the progress made during the last half century in understanding properties of polyampholyte solutions, their complexation with polyelectrolytes, and interaction of polyampholytes with surfaces and interfaces. We begin our discussion of this subject by describing the properties of aqueous polyampholyte solutions.

POLYAMPHOLYTE SOLUTIONS

Experimental Studies of Polyampholyte Solutions

The first study of synthetic polyampholytes was reported by Alfrey, Morawetz, Fitzgerald, and Fuoss[11] in their 1950 article "Synthetic Electrical Analog of Proteins." Since that time, a number of researchers have confirmed the *five basic findings for dilute polyampholyte solutions*.

Correspondence to: A.V. Dobrynin (E-mail: avd@ims.uconn.edu)

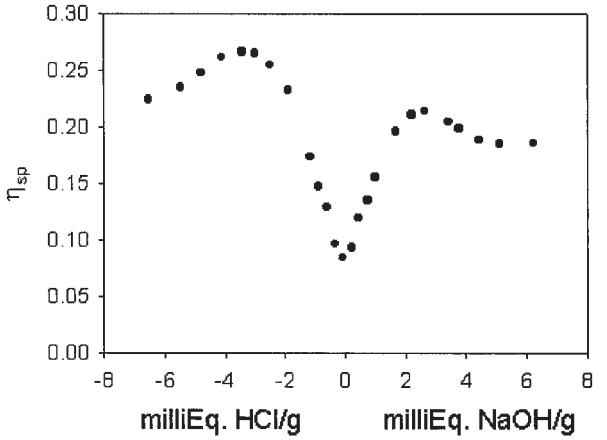

Figure 1. Dependence of the specific viscosity on added acid or base in a dilute (1 g/dL) solution of a synthetic random copolymer of 62% 2-vinyl pyridine and 38% methacrylic acid in 90% methanol and 10% water at 30 °C.[13] As prepared, this polyampholyte is at the isoelectric pH (the zero on the abscissa) where the viscosity has a minimum.

1. The conductivity, viscosity and coil size of weakly hydrophobic polyampholytes have minima at the isoelectric pH,[12–18] and a negative second virial coefficient.[19] The minimum in viscosity is seen in Figure 1, for a random copolymer of 62% 2-vinyl pyridine and 38% methacrylic acid in a solvent that is 90% methanol and 10% water.[13]
2. Hydrophobic polyampholytes precipitate in the vicinity of the isoelectric pH.[12,20,21] The copolymer in Figure 1 does not dissolve in pure water, but will dissolve in either aqueous acid (pH $<$ 3.7) or aqueous base (pH $>$ 7.3).
3. The viscosity and coil size increase as salt is added to the nearly charge-balanced polyampholyte solution.[18,19,21–28] The increase in viscosity with added salt is shown in Figure 2, for 2.8 $<$ pH $<$ 3.7 for a cellulosic polyampholyte.[18]
4. The viscosity and size decrease as salt is added for polyampholytes with a large net charge (the polyelectrolyte regime).[14,21,27,28] This decrease is shown in Figure 2 at the highest and lowest pH. At either very high or very low pH, polyampholytes act like polyelectrolytes.[29,30] This effect is also evident in Figure 1, where viscosity decreases with either excess acid or excess base. Once ionization is complete, addition of more acid or base simply increases the ionic strength of the solution.
5. The viscosity and coil size in pure water display a strong minimum as a function of copolymer composition, where positive and negative charges are balanced.[17,21,25]

Swelling of polyampholyte gels parallels the size change of polyampholyte chains in solution.[31,32] Swelling increases weakly as salt is added to an isoelectric gel, and decreases strongly as salt is added to a charge-imbalanced gel (analogous to polyelectrolyte gels).

Katchalsky and Miller[20] studied the influence of oppositely charged groups on dissociation, and found that increasing the acid content of their copolymers caused a larger fraction of the basic monomers to dissociate at a given pH, and presented a simple theory for this observation. As expected, addition of salt diminishes this inductive influence of neighboring groups, through simple screening of electrostatic interactions. Indeed, Katchalsky and coworkers[33–35] formulated a full theory of dissociation in charged polymers in the 1950s, which stands today as the seminal work in the field. This model has recently been reviewed and compared with experimental data.[1]

Salamone, Watterson, and coworkers at the University of Lowell prepared and studied polyampholytes with a wide variety of chemistries.[22,23,26,36,37] The results from those studies were very similar to the results from the 1950s described above. Their 1988 work was the most

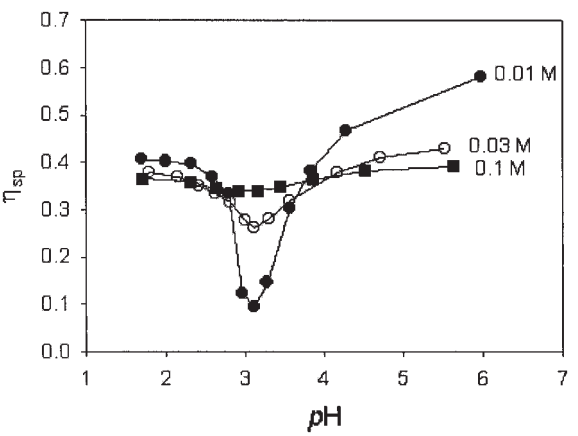

Figure 2. Specific viscosity of a dilute (0.060 g/dL) cellulosic polyampholyte as functions of pH and NaCl concentration at 25 °C.[18] The lines are simply guides for the eye, connecting the points for the three different NaCl concentrations.

thorough study of polyampholyte solution rheology to date, in which they focused on the shear rate dependence of apparent viscosity.[22] Here, they studied equimolar copolymers of x mol % 3-methacrylamidopropyltrimethylammonium (MPTMA), x mol % 2-acrylamido-2-methylpropanesulfonate (AMPS) with (100 − 2x) mol % acrylamide, and also y mol % 2-methacryloyloxyethyltrimethylammonium (METMA), y mol % 2-methacryloyloxyethane-sulfonate (MES) with (100 − 2y) mol % acrylamide. Parameters x and y were varied from roughly 1 to 6.5 mol % and the molecular weights of all polymers were quite high ($10^6 < M < 15 \times 10^6$). Interestingly, they found that both the magnitude of the apparent viscosity and its dependence on shear rate *decreased* as the fraction of charged groups increased. This important observation was subsequently confirmed on another system by McCormick and Johnson,[39] and is expected because the size of the polyampholyte should decrease as more charged groups are added.

McCormick and coworkers at the University of Southern Mississippi have been the leaders in the field in recent years.[21,25,27,39–43] In addition to the many confirmations of the classical findings for dilute polyampholyte solutions discussed above, these workers also discovered a new twist for dilute solutions. For charge imbalanced polyampholytes (in the polyelectrolyte limit) the viscosity first decreases as salt is added and then increases as more salt is added (as in the polyampholyte limit).[39,42] Modern theories of polyampholytes expect this behavior, as salt first screens the charge repulsion on large scales that extends the chain, and only at higher salt concentrations the charge attraction, that compacts the polyampholyte locally, is screened, causing the chain to swell.[44,45] An analogous effect has recently been reported for the salt dependence of polyampholyte gel swelling.[46]

The only experimental data on higher concentration (semidilute) polyampholyte solutions are the studies by Peiffer and Lundberg[47] and by McCormick and Johnson.[25,39] Peiffer and Lundberg[47] reported a very strong concentration dependence of viscosity (either exponential or a power law with $\eta \sim c^7$). However, the polymers they studied were weakly charged, with considerable hydrophobic character which is likely responsible for the strong concentration dependence (due to intermolecular associations between polyampholyte chains). Gelatin is primarily composed of hydrophilic amino acid monomers and does not

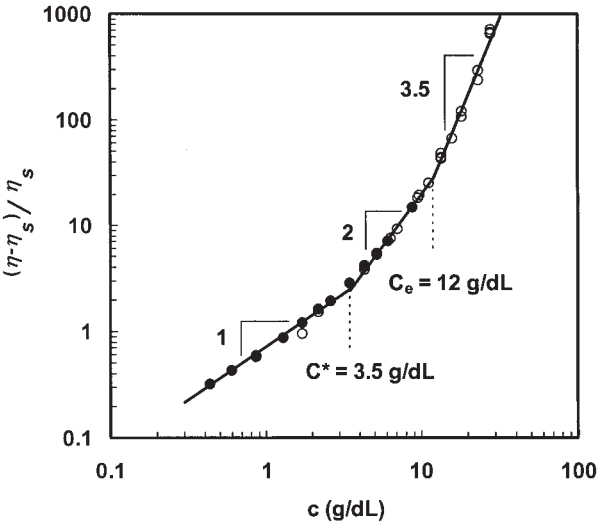

Figure 3. Specific viscosity of gelatin solutions[38] at 45 °C and pH = 5.7. Gelatin is a random coil (denatured) form of the protein collagen. Below the overlap concentration c*, specific viscosity is proportional to concentration. For semidilute unentangled solutions ($c^* < c < c_e$) specific viscosity scales as the square of concentration. Above the entanglement concentration c_e, specific viscosity scales as the 3.5 power of concentration.

exhibit such a strong concentration dependence, as shown in Figure 3, where the strongest concentration dependence is $\eta \sim c^{3.5}$. McCormick and Johnson[25,39] investigated only the low concentration end of the semidilute regime, where no entanglement effects are expected, and found a slightly stronger than linear concentration dependence of viscosity.

An important point regarding the composition distribution of randomly prepared polyampholytes was explored in detail by Candau and coworkers.[48–50] Strongly hydrophobic polyampholytes with an average balanced charge stoichiometry are fully soluble in the presence of excess salt. Polymers that are truly charge-balanced precipitate from solutions with lower salt concentrations, leaving only the highly extended charge-imbalanced chains in solution. Thus, salt can, in some cases, provide a means of fractionation.

Another interesting class of polyampholytes is the zwitterionic (or betaine) polymers with both positive and negative charges on the same monomer.[51,52] These polymers are dominated by attraction between monomers, which generally makes them insoluble in pure water. However, the attraction is screened as salt is added, allowing the zwitterionic polymers to dissolve. The

amount of salt required to dissolve the polymer has been found to depend on monomer structure, pH, and the particular salt used.[1,44,53–55] Once soluble, the zwitterionic polymers intrinsic viscosity,[53,56–61] hydrodynamic size,[56,58,62] radius of gyration,[58] and second virial coefficient[56] all increase as salt is added. The addition of salt screens the attraction between monomers, and at a particular salt concentration, the second virial coefficient is zero[56] and the intrinsic viscosity is proportional to the square root of molecular weight (a θ-condition). With certain zwitterionic polymers[56,63] the salt dependence of hydrodynamic size first shows an abrupt decrease before the usual increase in size with added salt. This is most likely caused by intermolecular aggregates being broken apart by screening the attraction between chains with small amounts of added salt. In crosslinked zwitterionic gels,[45,64] swelling increases as salt is added, consistent with the expected screening of attraction between monomers. Such zwitterionic gels have potential for chromatographic separation of proteins.[65,66]

Models of Polyampholyte Chains in Dilute Solution

Charge Distribution along a Polyampholyte Chain

Properties of polyampholyte chains in solutions depend not only on the average composition—the fractions of positively charged f_+ and negatively charged f_- monomers—but also on the distribution of charged monomers along the polymer backbone. This distribution of charged monomers is fixed during the polymerization reaction, and is known as a quenched charge distribution. A charge-balanced (net neutral or symmetric) polyampholyte with degree of polymerization N has equal numbers of positively f_+N and negatively f_-N charged groups. The net charge or charge asymmetry δfN of a polyampholyte is equal to the absolute value of the difference between numbers of positive f_+N and negative f_-N charges ($\delta fN = |f_+N - f_-N|$).

The distribution of charged monomers along the backbone of a polyampholyte chain that has no neutral monomers can be described by a 2×2 transfer matrix $p_{\alpha\beta}$. The matrix elements $p_{\alpha\beta}$ give conditional probabilities that the $i+1$st monomer is of type α if the ith monomer is of type β. The conservation of the conditional probabilities imposes the following constraints on the matrix elements $p_{++} + p_{-+} = 1$, $p_{--} + p_{+-} = 1$ and average composition $f_+ = p_{++}f_+ + p_{+-}f_-$. Under these conditions, the transfer matrix $p_{\alpha\beta}$ has two eigenvalues 1 and $\lambda = p_{++} + p_{--} - 1$. The coefficient λ varies between $+1$ and -1. The parameter $\lambda = -1$ implies the following relations between conditional probabilities $p_{++} = p_{--} = 0$ and $p_{+-} = p_{-+} = 1$ and corresponds to an alternating charge sequence along the polymer backbone. In the case when the parameter $\lambda = 0$, all conditional probabilities $p_{\alpha\beta}$ are equal to 1/2. This corresponds to a random charge sequence where there are no correlations in positions of positive and negative charged groups. In this case, one can think of a charge sequence along the polymer backbone as a path of a random walker that can move forward and backward with equal probability. For charge-balanced polyampholytes this random walker should begin and end its trip at the origin and thereby maintain an equal number of steps forward and backward or equal number of positive and negative charges along the polymer backbone. For charge-unbalanced (asymmetric) random polyampholytes, this walker will end its path either to the left or to the right from the origin depending on the excess of positive or negative charges. If there are neutral monomers on the polymer backbone, a charge sequence is described using a 3×3 matrix of conditional probabilities.

However, even in the case of charge-balanced polyampholytes there are many different paths starting and ending at the origin that correspond to different charge sequences along the polymer backbone. Theoretical models as well as computer simulations described in the next sections usually consider ensemble average properties. This corresponds to averaging over all possible charge sequences along the polymer backbone with fixed fractions of charged groups and charge asymmetry. Consequently, the properties of the whole ensemble of chains are often represented by the properties of the most probable member, which may not always be valid.

For synthetic polyampholytes prepared by copolymerization reaction, the situation is even more complicated. In this case, one only has control over the composition of the initial monomeric mixture. Even for a symmetric mixture with equal concentrations of positive and negative monomers in the reaction bath, the polymers produced will have an excess of positively charged groups, negatively charged groups, or be neutral. The width of the charge asymmetry distribution is determined by the reaction rate constants be-

tween monomers that could favor either alternating, random, or blocky charge sequences.

The charge sequence of a polyampholyte chain consisting of weak basic and acidic groups can be adjusted by shifting the ionic equilibrium. This can be done either by changing the pH of the aqueous solution or by imposing an external electrostatic potential, for example, by placing chains near charged surfaces. Such polyampholytes are called annealed polyampholytes.

Charge-Balanced Polyampholytes

Qualitative understanding of the properties of polyampholyte solutions was developed in the work of Katchalsky and coworkers.[20] The first quantitative theory of the collapse transition of a single polyampholyte chain was proposed by Edwards, King, and Pincus (EKP).[67] They have shown that a charge-balanced (net neutral) randomly charged polyampholyte chain of N monomers, with equal numbers of dissociated f_+N positively charged monomers and f_-N negatively charged monomers, collapses into a globule (microelectrolyte) due to the Debye-Huckel fluctuation-induced attraction between charges, similar to that in simple electrolyte solutions.[68] The strength of the attractive interaction depends on the ratio of the Debye length of the corresponding electrolyte solution and the chain size. EKP argued that this collapse can be stabilized by the loss of entropy due to chain confinement to a smaller volume. The applicability of the Debye-Huckel theory for a randomly charged polyampholyte chain was justified by Dobrynin and Rubinstein[69] in the framework of the random phase approximation, and by Bratko and Chakraborty[70] in their Monte Carlo (MC) simulations.

Higgs and Joanny[71] showed that in the case of strong collapse, the more important stabilizing term is the third virial repulsion between monomers. They have calculated the size of a polyampholyte chain as a function of its degree of polymerization, number of positive and negative charges on it, and the salt concentration in solution. In particular, they have demonstrated that increasing the molecular weight of a polyampholyte in a dilute solution at constant charge fraction will always lead to its collapse into a globule, as observed experimentally.[1,22]

The origin of fluctuation-induced attraction is the electrostatic interaction between oppositely charged sections of a chain. Consider a randomly charged polyampholyte chain in a collapsed (globular) state. Such a chain can be viewed as a densely packed arrangement of concentration blobs with size ξ and number of monomers g. The blob size ξ separates two different ranges of length scales. At length scales smaller than the concentration blob size, the electrostatic interactions are too weak to perturb the chain conformation, and these chain sections still obey Gaussian statistics ($\xi^2 \approx b^2 g$). At length scales larger than the blob size ξ, electrostatic attractions force the chain to collapse. The local structure of a collapsed polyampholyte chain resembles that of a dense electrolyte solution of blobs. Each positively charged blob is surrounded with higher probability by negatively charged blobs. The cohesive energy of a blob in such a solution is k_BT and is proportional to the energy of electrostatic interactions between two neighboring blobs carrying the typical charges eq and $-eq$, separated by a distance ξ.

$$F_{el}(g) \approx -k_BTl_Bq^2/\xi \tag{1}$$

The Bjerrum length $l_B \equiv e^2/(\varepsilon k_BT)$ is the distance at which the electrostatic interaction energy between two elementary charges e in a medium with dielectric constant ϵ is equal to the thermal energy k_BT. A blob of g monomers of a randomly charged polyampholyte chain has an average excess charge $eq = e(gf_+ + gf_-)^{1/2}$ (where gf_+ and gf_- are the average numbers of positive and negative charges inside a blob). Thus, the typical electrostatic energy between blobs is

$$F_{el}(g) \approx -k_BTl_Bgf/\xi \tag{2}$$

where $f = f_+ + f_-$ is the total fraction of charged monomers. At equilibrium, this electrostatic attraction is balanced by the three-body repulsion that is proportional to the thermal energy k_BT times the probability of three-body contacts [the product of the number of monomers in a blob g and the square of the volume fraction of monomers inside the blob $(\rho b^3)^2$], where ρ is the average monomer density inside the globule ($\rho \approx g/\xi^3$).

$$F_{rep}(g) \approx k_BTg(\rho b^3)^2 \approx k_BTg^3b^6/\xi^6 \tag{3}$$

The balance between three-body repulsion and electrostatic attraction determines the size of the blobs and the number of monomers in them.

$$\xi \approx b/(uf) \qquad g \approx (uf)^{-2} \tag{4}$$

We introduced the interaction parameter $u = l_B/b$—the ratio of the Bjerrum length l_B to the monomer length b. Equation 4 determines the polymer density inside a globule.

$$\rho \approx g/\xi^3 \approx ufb^{-3} \tag{5}$$

It is interesting to point out that the size ξ of a blob inside a globule is of the order of the Debye screening length due to charged groups on the polymer backbone.

$$r_D^{-2} = 4\pi l_B f\rho \approx b^{-2}(uf)^2 \approx \xi^{-2} \tag{6}$$

The screening of electrostatic interactions between fluctuating charges occurs at length scales of the order of the correlation blob size.

The globule with monomer density ρ has size[72]

$$R \approx (N/\rho)^{1/3} \approx b\left(\frac{N}{uf}\right)^{1/3} \tag{7}$$

As the fraction of charged monomers f on charge-balanced polyampholyte chain increases, the size of the globule decreases. The power law dependence of the globule size R on the fraction of charged monomers f for a polyampholyte globule (eq 7) is similar to the effective temperature dependence of the ordinary polymer globule, whose collapse is caused by attractive two-body monomer-monomer interactions ($R \sim \tau^{-1/3}$, where $\tau = \theta/T - 1$, see for review refs. 72 and 73). One can consider the fraction of charged monomers to be analogous to an effective temperature that is responsible for collapse of a polyampholyte chain. Increasing the fraction of charged monomers increases the strength of the fluctuation-induced electrostatic interactions and causes a stronger collapse of the polyampholyte chain. The electrostatic energy of a globule is equal to the number of blobs N/g times the contribution from each blob $F_{el}(g)$ (eq 2).

$$F_{glob} \approx -k_BT\frac{N}{g}\frac{l_Bgf}{\xi} \approx -k_BTu^2f^2N \tag{8}$$

There is another important contribution to the free energy of a polyampholyte globule: the surface energy. The origin of the surface energy is very simple. Each blob at the surface of the globule has fewer neighbors than blobs inside the globule have. Because two blobs inside a globule are interacting with energy of the order of the thermal energy k_BT, the energy cost for bringing a blob to the surface is also proportional to the thermal energy. There are S/ξ^2 blobs at the surface of the globule with surface area S, each contributing an additional k_BT to the total energy of the globule. This leads to the following estimate of the surface energy of a globule

$$F_{surf} \approx k_BT\frac{S}{\xi^2} \approx k_BT(uf)^{4/3}N^{2/3} \tag{9}$$

where the surface area S was estimated as R^2 (eq 7). The surface tension γ is the ratio of the surface energy F_{surf} and the surface area S and is of the order k_BT per area of blob ξ^2.

$$\gamma \approx \frac{F_{surf}}{S} \approx \frac{k_BT}{\xi^2} \approx k_BT(uf/b)^2 \tag{10}$$

A polyampholyte chain with size $R_0 \approx b\sqrt{N}$ collapses when the fluctuation-induced attraction energy F_{glob} becomes stronger than the thermal energy k_BT. This happens for sufficiently long polyampholyte chains $N > (uf)^{-2}$ (see eq 8). Figure 4(a) shows the collapse of symmetric polyampholytes as the degree of polymerization N increases, based on the simulations of Yamakov et al.[74]

The effect of the overall excess charge δQ on the ensemble averaged properties of polyampholyte chains was the central point of lattice Monte Carlo (MC) simulations of polyampholytes,[75–79] of off-lattice MC simulations of the bead-spring model of polyampholyte chains,[74,80] and of Molecular Dynamics (MD) simulations.[81,82] These simulations have shown that nearly charge-balanced random polyampholytes with charge asymmetry, δQ smaller than $e\sqrt{fN}$ (see next section for derivation of this condition), collapse into a globule as the temperature decreases. This collapse is caused by the fluctuation-induced attraction between charged monomers.

The effects of charge sequence on the collapse of charge-balanced polyampholytes were studied by lattice MC simulations.[83] Polyampholytes with an alternating distribution of charges behave like polymers with short-range interactions and can be characterized by an effective second virial coefficient.[85] The collapse transition of these polyampholytes is similar to the coil-globule transition of a neutral polymer.[83] The paper by Wittmer

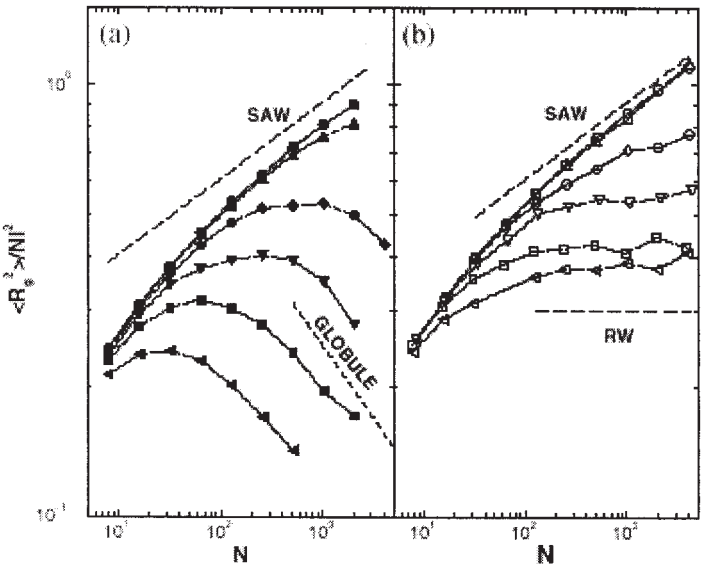

Figure 4. Radius of gyration R_g as a function of chain length N for (a) globally (full symbols) and (b) statistically (open symbols) neutral random polyampholytes. l_B/b = 1/64 (circles), 1/16 (triangles), 1/4 (diamonds), 1/2 (inverted triangles), 1 (open squares), 2 (sideways triangles). The data are normalized by the end-to-end distance of a random walk, while the straight lines indicate the slopes expected for self-avoiding walk ($R_g \propto N^{0.588}$), random walk ($R_g \propto N^{1/2}$), and globular ($R_g \propto N^{1/3}$) conformations (reproduced with permission from ref. 74).

et al.[85] has shown that the Debye-Huckel theory is inapplicable to strictly alternating polyampholytes because the charge pairs act as dipoles and large fluctuations of charge density are impossible (analogous to zwitterionic polymers). This leads to a fluctuation-induced attraction term that is quadratic in polymer concentration and a θ-point like collapse of a polyampholyte chain.

A qualitatively different picture of the collapse transition was discovered for diblock polyampholytes. Three separate regimes are identified in the electrostatically-driven coil-globule transition of flexible symmetric diblock polyampholytes.[84] In the first regime electrostatic attraction folds the chain by overlapping the two blocks, while each block is slightly stretched by self-repulsion. The second regime is dominated by the fluctuation-induced attractions between sections of oppositely charge strands stabilized either by short-range repulsion between monomers. The globule can be represented as a dense packing of correlation blobs. These blobs are analogous to the correlation blobs in a random polyampholyte globule. The size of a correlation blob for a symmetric flexible diblock polyampholyte is of the order of an electrostatic blob of individual polyelectrolyte blocks. The third regime starts by direct binding of oppositely charged groups, forming dipoles.[84] Dipoles associate into quadrupoles that can associate into larger multipoles. This regime leads to formation of multiplets analogous to those in ionomers.

The possibility of a freezing transition in random polyampholyte globules was investigated in computer simulations[86] and theoretically.[87] These works have established that because of the self-screening of electrostatic interactions in a polyampholyte globule, the freezing behavior of polyampholytes is qualitatively similar to the freezing transition in random heteropolymers with short-range interactions. The freezing transition for polymers with short-range interactions means that at low temperature it is impossible to minimize all interaction energies between monomers because of the additional constraint imposed by chain connectivity. Thus, at low temperatures the phase space of the system is divided into many subspaces corresponding to different chain configurations separated by high energy barriers. To go from one chain configuration to another, it is necessary to completely unfold and then fold the chain again. Among all states, there is one state that has energy much lower than the

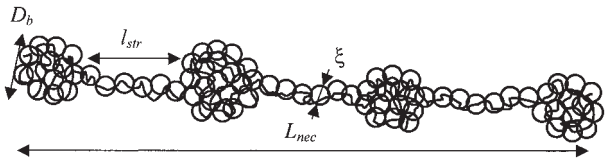

Figure 5. Schematic picture of a necklace globule, showing the bead size D_b, the string length l_{str}, the blob size ξ, and the necklace length L_{nec}.

others. This state is called the "native" state. In this native state a chain achieves the most optimal packing into a globule that minimizes the short-range interactions (see for review ref. 88).

Effect of Charge Asymmetry on Chain Conformations

The effect of net charge on the shape of a polyampholyte chain was studied by Kantor and Kardar,[75] by Gutin and Shakhnovich,[89] and by Dobrynin and Rubinstein.[69] Excess charge deforms the polyampholyte chain into an elongated globule similar to the well-known Rayleigh instability of a charged liquid droplet. Fluctuation-induced attraction collapses the chain into a globule, but the interplay of globule surface energy and repulsion of the net unbalanced charge elongates the globule.

A polyampholyte globule changes its shape when the energy of electrostatic interactions between excess charges $\delta Q = eN|f_+ - f_-|$ becomes comparable with the globular surface energy (Rayleigh's stability criterion).

$$\frac{l_B N^2 (f_+ - f_-)^2}{R} \approx \frac{R^2}{\xi^2} \tag{11}$$

For a randomly charged polyampholyte globule the critical net charge is equal to

$$\delta Q_{crit} \approx e\sqrt{fN} \tag{12}$$

Thus, collapsed polyampholytes with charge asymmetry $\delta fN = N|f_+ - f_-|$ smaller than $\sqrt{fN}$ maintain a roughly spherical shape, while polyampholyte globules with larger charge asymmetry $\delta fN > \sqrt{fN}$ are unstable. In the latter case, the elongation of the globule will reduce its total energy by lowering the energy of electrostatic interactions between excess charges at the expense of creating extra polymer–solvent interface. The change in globular shape occurs at a constant globular volume that is controlled by the fluctuation-induced charge attraction (eq 2) and three-body repulsive interactions (eq 3).

Polyampholytes with charge imbalance, δQ larger than $e\sqrt{fN}$, form a necklace globule (array of beads connected by strings) at low temperatures (see Fig. 5). There is a striking similarity between the instability of a polyampholyte globule with excess charge $\delta Q \approx e\sqrt{fN}$ and the necklace instability of a polyelectrolyte chain in a poor solvent.[90–95] However, for polyampholytes, the factors responsible for the shape of a globule are all electrostatic in nature. The number of monomers m_b in each bead of size D_b is determined by Rayleigh's stability condition—the surface energy of a bead γD_b^2 is of the order of its electrostatic energy.

$$\gamma D_b^2 \approx k_B T (uf)^2 \frac{D_b^2}{b^2} \approx \frac{(e\delta f m_b)^2}{\varepsilon D_b} \tag{13}$$

The surface tension γ was estimated using eq 10, and δf is the charge asymmetry ($\delta f = |f_+ - f_-|$). For beads with density ρ, the number of monomers in a bead m_b and its size D_b are connected as $D_b \approx (m_b/\rho)^{1/3}$. Substitution of this relation (and eq 5 for ρ) into eq 13 results in the number of monomers in a bead.

$$m_b \approx f/(\delta f)^2 \tag{14}$$

There is more than one bead on a chain when the number of monomers in a bead m_b is smaller than the number of monomers on a polyampholyte chain N. The number of monomers in a bead increases as the charge asymmetry δf decreases. Because this transformation occurs in a single chain, all these beads are connected by strings of blobs of size ξ (eq 4), forming a pearl necklace. The equilibrium length of strings l_{str} between beads is obtained by equating the surface energy of a string $\gamma\xi l_{str}$ with the electrostatic repulsion between two neighboring beads.

$$\gamma\xi l_{str} \approx k_B T \frac{l_{str}}{\xi} \approx k_B T (uf) \frac{l_{str}}{b} \approx \frac{(e\delta f m_b)^2}{\varepsilon l_{str}} \tag{15}$$

The string length l_{str} is estimated by solving eq 15, making use of eq 14.

$$l_{str} \approx b\sqrt{f}/\delta f \approx b\sqrt{m_b} \tag{16}$$

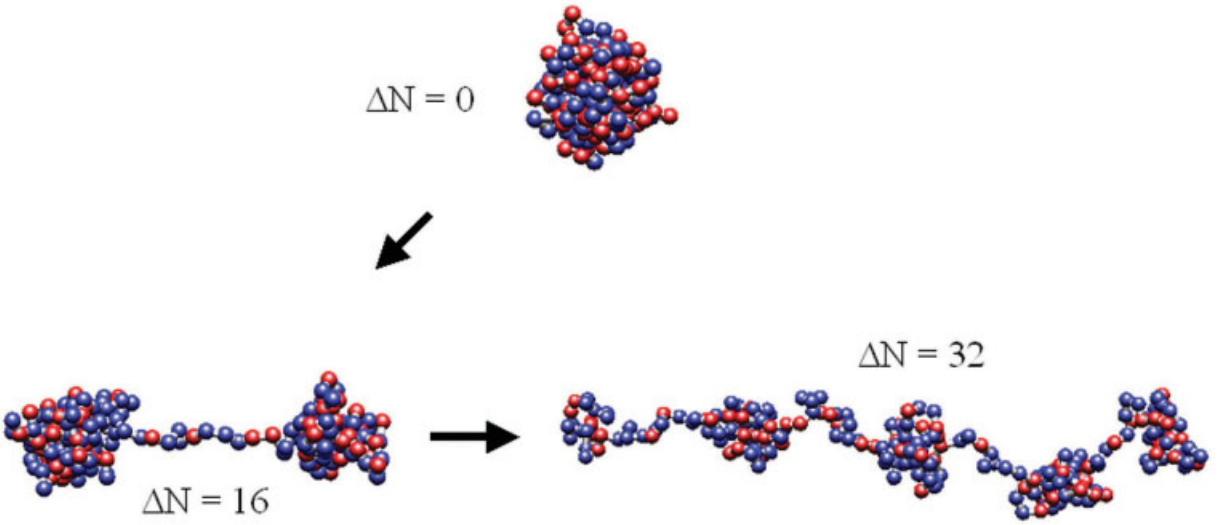

Figure 6. Cascade of transitions in a polyampholyte chain as a function of the charge asymmetry $\Delta N = \delta fN$, for a polyampholyte chain with $N = 256$ and the value of the interaction parameter $u = 3$. Provided by J. Jeon.

The string length increases as the charge asymmetry decreases. Decreasing the charge asymmetry causes the beads to grow (see eq 14), accumulating a bigger charge. This large charge forces strings to increase in length to offset the electrostatic repulsion between two neighboring beads. In the case when most of the necklace mass is stored in beads and the strings are longer than the bead diameter, the size of the necklace can be estimated as the number of beads on a chain N/m_b times the string length l_{str}

$$L_{nec} \approx \frac{l_{str}N}{m_b} \approx b\frac{\delta fN}{\bar{f}} \qquad (17)$$

The main difference between polyampholytes with large net charge and uniformly charged polyelectrolytes is the randomness in the charge sequence. For polyampholytes, the structure of the necklace is predetermined by the initial charge distribution. Monte Carlo studies by Kantor and Kardar[77,78] showed that the necklace might consist of a few almost neutral globules connected by charged necks, or even of one large almost neutral globule with a tail sticking out of it. A similar behavior was observed in simulations of ring-polyampholytes by Lee and Obukhov.[96]

The evolution of conformations for a random polyampholyte chain having degree of polymerization $N = 256$ as the charge asymmetry is increased is shown in Figure 6. A charge-balanced polyampholyte chain with zero net charge forms a globule. When the charge asymmetry $\Delta N = \delta fN = 16$ the globule splits into a dumbbell. As the charge asymmetry increases further, the chain adopts a necklace-like conformation of weakly charged beads connected by strings.

For an ensemble of random polyampholytes, the typical charge asymmetry of a chain δfN is proportional to $\sqrt{fN}$. Thus, the ensemble average necklace size in eq 17 should follow the ideal chain dependence on the degree of polymerization N ($L_{nec} \approx b\sqrt{N}$). This specific feature of the necklace model of polyampholyte chain was confirmed in the Monte Carlo simulations of Yamakov et al.[74] [see Fig. 4(b)] for long polyampholyte chains.

In summary, the overall size and shape of polyampholytes in dilute salt-free solutions is determined by the balance of four factors.[67,69–71,89]

1. Chain entropy tends to keep the polymer configuration as close to Gaussian statistics as possible.
2. Fluctuation-induced attractions between charges (similar to those observed in electrolyte solutions[68]) tend to collapse the chain into a globule.
3. Short-range three-body monomer-monomer interactions stabilize the size of the globule.
4. If the chain has a nonzero total charge (either positive or negative), the overall

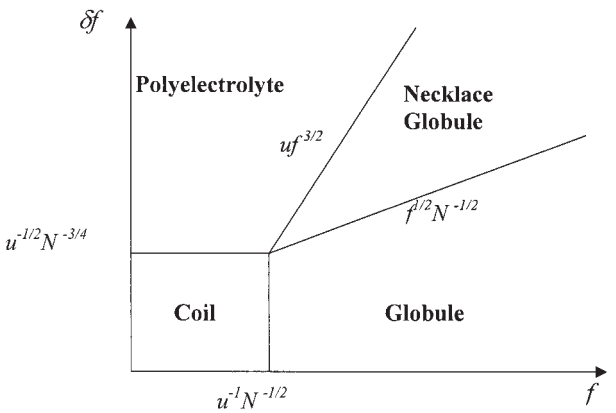

Figure 7. Diagram of states[97] of a polyampholyte chain in dilute solution in the parameter space of the total fraction of charged monomers $f = f_+ + f_-$ and the charge asymmetry $\delta f = |f_+ - f_-|$.

Coulomb repulsion between excess charges tends to elongate the chain.

The relative importance of these factors depends on the fraction of positive f_+ and negative f_- charges on the chain, on the charge sequence, on the degree of polymerization N, and on the ratio of the Bjerrum length l_B to the monomer size b, defining the relative strength of the electrostatic interactions ($u = l_B/b$). Figure 7 shows a diagram of states of a polyampholyte chain as a function of the charge asymmetry $\delta f = |f_+ - f_-|$ and total fraction of charged monomers $f = f_+ + f_-$.[97]

Effect of Added Salt on Chain Conformations

Salt ions can screen the repulsion between excess charges as well as the fluctuation-induced attraction between opposite charges.[69,71] In the polyelectrolyte regime with no added salt, the polyampholyte chain is stretched on its largest length scale by the repulsion between excess charges. As salt is added, the Debye length decreases and the repulsion between excess charges begins to be screened once the Debye length becomes smaller than the chain size. This screening of charge repulsion decreases the chain size. As more salt is added, the Debye length of the solution eventually decreases down to the internal polyampholyte Debye length due to the charged monomers, and further addition of salt screens the fluctuation-induced attraction, causing the chain to swell. The salt concentration c_s, at which the minimum polyampholyte size is attained, is determined by equating the two Debye lengths.

$$c_s \approx \frac{f\rho}{2} \approx \frac{uf^2}{2b^3} \tag{18}$$

In the polyampholyte limit, the size of a symmetric polyampholyte chain only increases with increasing salt concentration,[71] because the fluctuation-induced attraction between charged groups is screened by the salt ions. For a long enough polyampholyte in a good solvent for the backbone, there is always a critical salt concentration (analog of the ordinary θ-point for uncharged polymers) at which the net excluded volume is zero. This swelling of polyampholyte chains in the presence of salt ions was observed in recent molecular dynamics simulations.[98,99]

Equation 18 explains the minimum in salt concentration dependence of the solution viscosity of weakly charged polyampholytes with $f = 0.2$ and 0.3 at salt concentration $c_s = 0.1$ M NaCl observed by McCormick and Salazar.[42]

Phase Behavior of Polyampholyte Solutions

Synthetic polyampholytes are produced by random polymerization reactions. Such samples always contain chains with different fractions of positively and negatively charged groups. Everaers et al.[100,101] have argued that in solution, synthetic polyampholytes have a tendency for complexation, forming neutral complexes. The driving force for complexation between oppositely charged chains is the reduction of each chain's electrostatic self-energy. Such neutral complexes may further reduce their energy by forming larger neutral aggregates. The coalescence of two or more neutral complexes reduces the surface energy of the aggregate. For a neutral sample, for which the ensemble average charge asymmetry is equal to zero, concentrating the samples leads to a separation of an almost neutral precipitate and a supernatant containing counterions and almost neutral globules. For samples with asymmetric charge distributions, the supernatant contains highly charged globules while the precipitate remains neutral. This tendency for complexation between oppositely charged polyampholytes may be explored for sample fractionation by repeatedly dissolving and precipitating the neutral dense phase by adding and removing salt.

A complexation in polyampholyte solutions was studied in MD simulations by Tanaka and

Tanaka.[102] They found that a system of polyampholyte chains with zero net charge will phase separate from solution forming one huge globule— a cluster of several chains, structured similar to a concentrated polymer solution—as the strength of the Coulombic interactions increases (effectively decreasing the temperature T). In the case of a system of chains with nonzero net charge, the cluster of several chains swells to minimize the electrostatic repulsion between similarly charged monomers. The charged complexes of several chains broke apart when the net charge of the aggregate exceeded the critical value $\delta Q > e\sqrt{N}$ for the fully charged polyampholyte chains ($f = 1$). This is consistent with Rayleigh's instability criterion for the ensemble of chains.

The possibility of microphase separation in concentrated polyampholyte solutions was investigated in the framework of the random phase approximation by Gonzales-Mozuelos and Olvera de la Cruz for diblock polyampholytes,[103] and by Dobrynin for random polyampholytes.[104] These articles have shown that in concentrated polyampholyte solutions, the microphase separation is due to competition between short-range monomer–monomer attractive interaction favoring segregation of similar monomers and the Coulomb interaction between charged groups that opposes segregation. Placing opposite charges on the two blocks of a diblock copolymer stabilizes the disordered homogeneous phase lowering the temperature of microphase separation transition.

Effect of External Electric Field on Chain Conformations

The influence of uniform electric field on the dynamics and conformations of weakly charged polyampholyte chains was considered in a series of works.[82,105–110] It was established that the electric field pulls the oppositely charged monomers in opposite directions, polarizing the chain. As a result of these conflicting forces, the polyampholyte coil is stretched into a "tug of war" configuration. If the polyampholyte is in a globular state, the globule becomes unstable above a critical external electric field E_{C1} and breaks up forming a random necklace structure.[82] A polyampholyte collapses back into a globule as the strength of the external electric field E is lowered below E_{C2}. The strength of the electric field E_{C2} at which a polyampholyte collapses back into a globule is weaker than one required to break up a globule E_{C1} ($E_{C2} < E_{C1}$). There is a hysteresis in chain size dependence on the external electric field. This hysteresis is a manifestation of the coexistence of two states of a dilute polyampholyte chain—collapsed and elongated—separated by a barrier.

POLARIZATION-INDUCED ATTRACTION AND POLYAMPHOLYTE ADSORPTION

Experimental Studies of Polyampholyte Adsorption—The Gelatin Example

Many experimental studies of polyampholyte adsorption were stimulated by the need of the photographic industry to understand and control gelatin adsorption at charged surfaces.[111,112] Gelatin is a polypeptide copolymer (denatured protein) consisting of neutral, basic, and acidic amino acid groups. Depending on whether the solution pH is above or below the isoelectric point (IEP) of gelatin pH(IEP) = 4.9, the molecule can be anionic or cationic. From the results on the competitive adsorption of a cyanine dye, Curme and Natale[113] concluded that gelatin adsorbs onto silver bromide particles and that maximum adsorption occurs around the IEP. The data on the heat of adsorption by Berendsen and Borginon[114] indicated that the binding energy increases at pH values below the IEP and remains roughly constant above the IEP. The adsorption isotherms of gelatin on AgBr both above and below the IEP were measured by Kragh and Peacock.[115] Direct surface force measurements between adsorbed gelatin layers on mica at various ionic strengths and solution pH were reported by Kawanishi et al.[116] and by Kamiyama and Israelachvili.[117] These studies show that gelatin adsorbs via discrete ionic bonds formed between negative surface groups on mica and positive basic groups on gelatin. The gelatin still adsorbs even when it has net negative charge of the same sign as the charge on the mica surface. Similar trends in the adsorption of synthetic polyampholytes on charged latex particles have been observed by Neyret et al.[118]

Model of Single Chain Adsorption

Recent theoretical studies[97,119–123] and computer simulations[124,125] revealed a new mechanism of polyampholyte adsorption that is due to polarization of chains in the external electric field created by a charged object.

Consider the adsorption of a single weakly charged polyampholyte chain with fraction of charged monomers $f < u^{-1} N^{-1/2}$ (in this case the fluctuation-induced attractive interactions are weak and the chain keeps its unperturbed Gaussian conformation) onto an infinite plane with σ charges per unit area. In the absence of added salt, the electric field $E(z)$ decays with distance z from the surface as

$$E(z) = \frac{4\pi e\sigma}{\varepsilon} \frac{\lambda}{\lambda + z} \tag{19}$$

where $\lambda = (2\pi l_B \sigma)^{-1}$ is the Gouy-Chapman length.

The size $D(z)$ of a random polyampholyte chain at distance z from the charged surface can be estimated by balancing the electrostatic energy of the dipole of two opposite charges $(fN)^{1/2}$ of the two halves of the chain separated by the distance $D(z)$ in the external electric field $E(z)$ with the chain elastic energy.

$$E(z) e \sqrt{fN} D(z) \approx k_B T \frac{D(z)^2}{b^2 N} \tag{20}$$

This balance leads to the size of the chain in the direction perpendicular to the surface.

$$D(z) \approx \frac{E(z) e f^{1/2} N^{3/2} b^2}{k_B T} \approx \frac{R_0^2 \sqrt{fN}}{z + \lambda} \tag{21}$$

where $R_0 = bN^{1/2}$ is a Gaussian chain size.

At distances z from the surface shorter than the Gouy-Chapman length λ, the size of the chain perpendicular to the surface grows linearly with the surface charge density σ.

$$D \approx \frac{R_0^2 \sqrt{fN}}{\lambda} \approx l_B R_0^2 \sqrt{fN} \sigma, \qquad for \quad D < \lambda. \tag{22}$$

This is the so-called *pole regime*. The electric field of the charged surface induces elongation of the chain in the direction of the field [see Fig. 8(a)], while in the perpendicular direction the chain keeps its Gaussian conformation. The chain is significantly elongated ($D > R_0 = bN^{1/2}$) when the surface charge density exceeds the value

$$\sigma_1 \approx (l_B b f^{1/2} N)^{-1} \approx (l_B R_0 \sqrt{fN})^{-1} \tag{23}$$

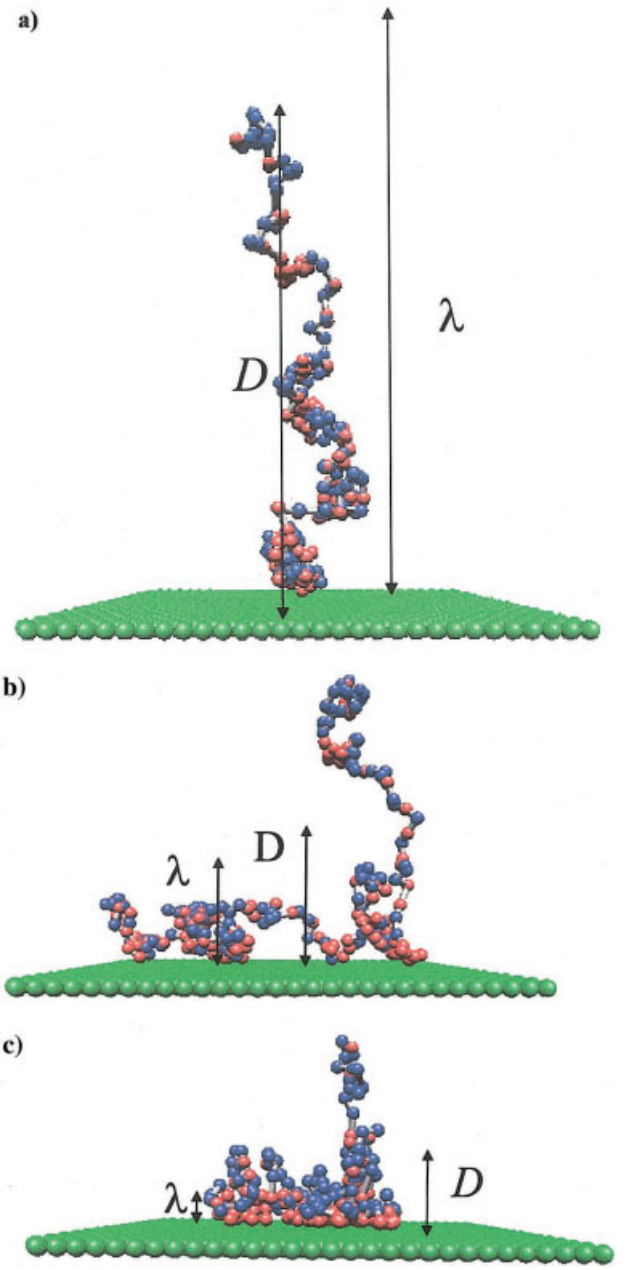

Figure 8. Conformation of a polyampholyte chain near an adsorbing surface. (a) Pole regime. (b) Fence regime. (c) Pancake regime.

For example, for a chain with $N = 500$ monomers, with charged monomer fraction $f = 0.02$, and with the monomer length $b = 3$ Å in a solution with Bjerrum length $l_B = 7$ Å, the adsorption threshold is at $\sigma_1 \approx 7 \times 10^{-4}$ charges/Å^2 and the value of the Gouy-Chapman length at this adsorption threshold is $\lambda_1 \approx b f^{1/2} N \approx 200$ Å.

The polarization energy of a polyampholyte chain in the external electric field is

$$W(z) \approx -e\sqrt{fN}D(z)E(z) \approx -k_BT\left(\frac{\lambda_1}{z+\lambda}\right)^2 \quad (24)$$

At larger distances from the surface $z > \lambda_1$, the small polarization energy gain does not justify the conformational entropy loss due to stretching of the chain, and the polymer keeps its Gaussian conformation. At these distances, the attraction energy between the chains and the surface is less than the thermal energy k_BT and the chains move freely through the solution.

The size of the chains near the wall D increases with increasing surface charge density and becomes the same order of magnitude as the Gouy-Chapman length λ, when the surface charge density σ reaches the value σ_2

$$\sigma_2 \approx (l_B b f^{1/4} N^{3/4})^{-1} \approx (l_B R_0 (fN)^{1/4})^{-1} \quad (25)$$

For our example with $N = 500$, $f = 0.02$, $l_B = 7$ Å and $b = 3$ Å, the charge density $\sigma_2 \approx 10^{-3}$ charges/Å^2 and the corresponding Gouy-Chapman length $\lambda_2 \approx 120$ Å. At higher surface charge densities $\sigma > \sigma_2$, the system crosses over to the *fence regime*. The chain in this regime remains confined within the Gouy-Chapman length and is divided into subsections of size λ [see Fig. 8(b)]. These subsections are strongly stretched and the polymer is strongly attracted to the surface. In this regime, the chain size decreases with increasing surface charge density.

As the surface charge density increases further, the Gouy-Chapman length λ decreases and the system crosses over to the *pancake regime* at the surface charge density

$$\sigma_3 \approx f^{1/2}/(l_B b) \quad (26)$$

In the pancake regime ($\sigma > \sigma_3$), all monomers with charge sign opposite to that of the surface are within distance λ of the surface, while the monomers with charge of the same sign as the surface are in the loops dangling in solution at distances larger than λ [see Fig. 8(c)]. The average size of the loops can be estimated by comparing the repulsive force between the surface and the charges located at distance z from the surface (k_BT/z) with the elastic force of a strand of f^{-1} monomers (k_BTzf/b^2). At equilibrium these two forces are equal. This leads to the condition of almost unperturbed strands of size $bf^{-1/2}$. The polarization energy of the chain section with f^{-1} monomers is of the order of the thermal energy k_BT. The gain of attraction energy due to reorganization of monomers in the adsorbed layer is k_BT per loop. For the above example $\sigma_3 \approx 10^{-2}$ charges/Å^2 and the corresponding Gouy-Chapman length $\lambda_3 \approx 20$ Å.

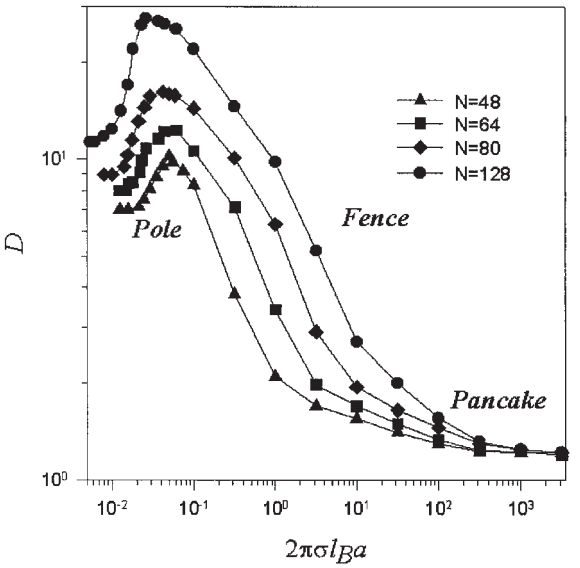

Figure 9. Nonmonotonic dependence of the thickness D of the adsorbed polyampholyte chain on the surface charge density σ (logarithmic scales).

The polarization-induced attraction mechanism for chain adsorption also allows adsorption of polyampholyte chains carrying the same sign of net charge as the charge of the adsorbing surface.[97,119,126]

Figure 9 shows the results of Monte Carlo simulations of adsorption of polyampholyte chains with degrees of polymerization $N = 32$, 48, 64, 80, and 128 and with equal numbers of positively and negatively charged monomers at a charged surface from a θ-solvent for the polymer backbone.[127] The properties of adsorbed polyampholyte chains were averaged over 100 different charge sequences. It is important to point out that the change in chain conformation near the adsorbing charged surface described above is not only happening to a chain that is in physical contact with the adsorbing surface. The long-range nature of polarization-induced attractive interactions leads to polarization of chains that are not in physical contact with the adsorbing surface. For example, in the range of surface charge densities corresponding to the pole regime, all chains with center of mass located within the distance λ_1 from the adsorbing surface have a polarization energy that is larger than the thermal energy k_BT. Thus, the

choice of adsorbed chains based on the energetic criteria selecting chains with the polarization energy much larger than the thermal energy k_BT will actually count all chains within a layer of thickness λ_1 as adsorbed chains. Another selection criteria used in simulations of neutral chain adsorption is based on the position of the center of mass with the usual cutoff distance being of the order of the Gaussian chain size for adsorption from a θ-solvent. This works for neutral chains because the attractive interactions between the surface and the polymer are short ranged and confine the adsorbed chains within a thickness smaller than the Gaussian size of the chain. However, this method does not work for polyampholytes in the pole regime and in part of the fence regime, where chains are stretched beyond their Gaussian size. For example, a chain in the pole regime with size larger than the Gaussian chain size can have its center of mass outside the distance $bN^{1/2}$. Setting the cutoff at the Gaussian chain size actually eliminates all chains that are in the strongly stretched pole regime. This was done in the Monte Carlo simulations conducted by Khan et al.[128] As a result of this selection method, the authors observe a weak chain size dependence on the degree of polymerization in the pole regime, $D \sim N^{0.7}$. This weak dependence is not surprising because the selected cutoff eliminated all strongly polarized chains for which the chain size scales with number of monomers N as $D \sim N^{1.5}$. The crossover to the fence regime and the chain size dependence in the fence regime were also misinterpreted.

To avoid all these problems with identifying adsorbed chains, for each charge sequence a distribution of chain sizes as a function of the position of the center of mass can be determined. All chain conformations for which the center of mass of the chain is located within two radii of gyration in the z-direction should be included in the ensemble averages. Computer simulations based on this analysis protocol qualitatively confirmed the predictions of the scaling model[97,119] but pointed out a number of important corrections to scaling.

The onset of adsorption occurs at a low surface charge density that is almost inversely proportional to the degree of polymerization N ($\sigma_1 \sim N^{-0.93\pm0.05}$) as expected by eq 23. The chain thickness increases with surface charge density in the pole regime, with the exponent approaching unity for large N (see Fig. 9). However, when the charge density reaches a critical value $\sigma_2 \sim N^{-0.73\pm0.04}$ (see eq 25), the ensemble average polymer thickness D peaks, thus marking the beginning of the qualitatively different fence regime.[127]

In the fence regime, the ensemble average thickness D of the adsorbed chain decreases with increasing surface charge density and eventually saturates at very high charge densities. The decrease of thickness D with the surface charge density σ is slower than predicted by the scaling model due to finite size effects. At sufficiently high charge densities, the charges on polyampholyte chains opposite in sign to those of the wall find it highly preferable to be in close proximity to the wall (within a distance of the order of the Gouy-Chapman length). This effect leads to the formation of a series of loops with charges of one sign separated by trains of opposite charges pinned to the wall—the pancake regime. This regime starts when the Gouy-Chapman length is of the order of the distance between charged monomers. Consequently, the thickness of the ensemble of adsorbed chains in the pancake regime is of the order of the loop size between nearest similarly charged monomers along the polymer backbone and universal for all N (see Fig. 9).[127]

Multichain Adsorption and Structure of the Adsorbed Layer

The long-range polarization-induced attraction between polyampholyte chains and the charged surface, leads to multiple adsorbed polymer layers. The structure and thickness of these adsorbed layers depends on the charge distribution along the polyampholyte backbone (which determines the polarizability of polyampholyte chains in external electric fields[105–108]), solution concentration and features of the adsorbing surface such as its curvature and surface charge density. The equilibrium polymer density profile in the adsorbed layer is determined by the balance of the long-range polarization-induced attraction of a polyampholyte chain to the charged object (see eq 24) and the monomer–monomer repulsion. In the case of a θ-solvent for the polymer backbone, the monomer–monomer repulsive interactions are controlled by three-body contacts. For a polymer chain located at distance z from the charged surface at polymer concentration $\rho(z)$, the number of three-body contacts per chain is equal to the probability of three-body contacts per monomer $(\rho(z)b^3)^2$ times the number of monomers per chain N. Each three-body contact contributes the order of the thermal energy k_BT to the chain's free

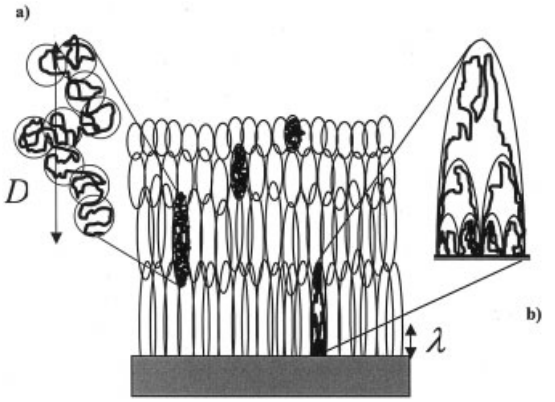

Figure 10. Schematic of the structure of adsorbed polyampholyte chains. Inset (a) stretched adsorbed chain in the multilayer, and inset (b) self-similar pseudobrush layer at the surface.

energy. At equilibrium, the energy of three-body interactions between monomers $k_BTNb^6\ [\rho(z)]^2$ is of the order of the chain polarization energy given by eq 24.

$$k_BTNb^6[\rho(z)]^2 \approx k_BT\left(\frac{\lambda_1}{z+\lambda}\right)^2 \tag{27}$$

Solving this equation for the polymer density one obtains the following expression for the polymer density profile in the adsorbed layer.

$$\rho(z) \approx \frac{1}{b^3N^{1/2}}\left(\frac{\lambda_1}{z+\lambda}\right) \tag{28}$$

At large distances ($z > \lambda$), the polymer density is inversely proportional to the distance z from the adsorbing surface. This is a direct result of long-range attractive interactions between the polyampholyte chain and the adsorbing surface. In fact, the adsorbed layer can be much thicker than the size of individual chains (see Fig. 10). The detailed structure of the adsobed layer was obtained in the framework of self-consistent mean-field and scaling approaches (see for details refs. 120, 122, and 129). According to these studies, the adsorbed chains may form a multilayer of stretched chains further away from the surface [see Fig. 10(a)] and a self-similar pseudobrush layer at the surface [see Fig. 10(b)]. The pseudobrush layer structure is a result of the local balance of the polarization energy of the chain strand with $g(z)$ monomers and size z

$$F_{\text{polar}} \approx -ze\sqrt{fg(z)}E(z) \tag{29}$$

where the electric field $E(z)$ near the charged surface is given by eq 19, its elastic energy

$$F_{\text{el}} \approx k_BTz^2/(b^2g(z)) \tag{30}$$

and the three-body interactions of this strand with surrounding chains

$$F_{\text{rep}} \approx k_BTg(z)b^6[\rho(z)]^2. \tag{31}$$

At equilibrium, all three terms are of the same order of magnitude. This allows us to find the relations between the number of monomers in a chain strand $g(z)$, polymer density profile $\rho(z)$ and distance z from the adsorbing surface. In this layer, the polymer density shows a much weaker dependence on the distance z from the adsorbing surface.

$$\rho(z) \approx b^{-3}\left(\frac{bf}{\lambda+z}\right)^{1/3} \tag{32}$$

The thickness of this self-similar layer is of the order of λ_2, which corresponds to a loop formed by the whole polymer chain. The adsorption stops at distances from the adsorbing surface where the external electric field created by the charged surface is not strong enough to polarize the polyampholyte chain ($H \approx \lambda_1$).

The adsorption of polyampholyte chains at a charged spherical particle is qualitatively similar to the adsorption at planar surfaces. The only difference between those two cases is the distance dependence of the electric field created by charged spheres. In the case of a spherical particle, the electric field $E(r)$ is proportional to r^{-2}, leading to a faster decay of the polymer density with distance r from the center of a particle. The structure of the first layer of adsorbed chains resembles that of a star polymer (see for details[121–123]).

Experimental Verification of the Multichain Adsorption Model

This theory of polyampholyte adsorption on charged surfaces was successful in interpretation of experimental results for adsorption of gelatin on polystyrene latex and silica particles at various pH and ionic strengths.[130] In these experiments the hydrodynamic diameter D_h of the particles was determined as a function of gelatin

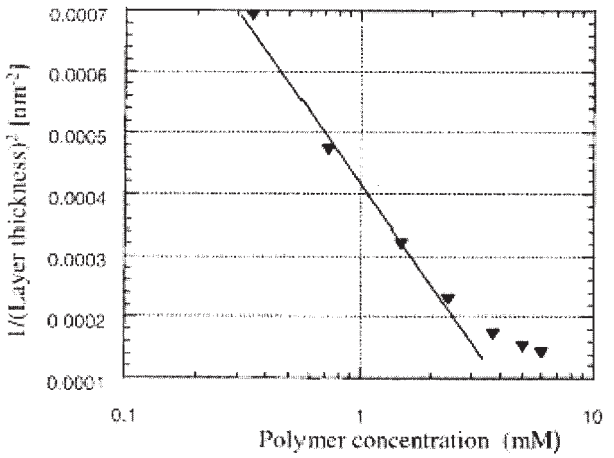

Figure 11. Adsorption isotherm for gelatin onto negatively charged polystyrene latex particles at pH = 5.5 (experimental data from ref. 130). Solid line—theoretical prediction.

solution concentration c_B from the measurements of the apparent diffusion constant of the particles with an adsorbed gelatin layer and the viscosity of the latex/gelatin solution. The thickness of the adsorbed gelatin layer H was estimated by subtracting the hydrodynamic diameter of a bare particle $D_h^0 = 135$ nm from the diameter D_h of the particle covered with gelatin. The polystyrene particles were negatively charged with surface charge density $\sigma = 1/82$ charges/Å^2. The behavior of gelatin in aqueous solutions indicates that it is an annealed polyampholyte with pH-dependent charge on the chains. Adsorption of such polymers is accompanied by adjustment of their charge (the external electrostatic potential created by adsorbing particle shifts locally the ionic dissociation equilibria), and therefore ionization of the adsorbed molecules (and net charge δfN) will vary with distance z from the adsorbing particle. For the bulk solution with pH = 5.5 and no added salt, the isoelectric point is located within the adsorbed layer at $z_{iso} = 20$ nm.

Figure 11 shows the experimental dependence of the reciprocal square layer thickness H^{-2}, on the logarithm of gelatin concentration $\ln(c_B)$ with the upper boundary for gelatin extended to $c_B < 7$ mM. According to the prediction of the scaling model, one expects in these coordinates a straight line with slope of the order of $\lambda_1^{-2} \approx (b^2 fN^2)^{-1}$. The experimental data can be fitted reasonably well by a line of slope -6.25×10^{-4} nm^{-2} (shown by the solid line). As the solution concentration approaches the overlap concentration, the experimental points deviate from the theoretical curve. This is not surprising, because the scaling model is based on the expression for the chemical potential of polyampholyte molecules in *dilute* solutions. The value of the slope estimates the parameter $\lambda_1 \approx bf^{1/2}N \approx 40$ nm. For a gelatin chain with $N = 1000$ monomeric units and monomer size $b = 3$ Å, we can estimate the fraction of ionized groups on a gelatin molecule f to be equal to $f = 1.9 \times 10^{-2}$. Thus, the model expects about 20 charges per each gelatin chain. This estimation of the total number of charged amino acids on a gelatin molecule is one order in magnitude smaller than the total number of ionizable amino acids (about 200) on a gelatin molecule. The origin of this discrepancy remains an open question.

The adsorption isotherm of the gelatin/polystyrene latex system was studied by Vanberg et al.[131] Here, the adsorption of gelatin on latex particles was monitored by a fluorescence technique. The polystyrene particles had hydrodynamic radius $R_h^0 = 37$ nm and surface charge density $\sigma = 1/148$ charges/Å^2. This surface charge density corresponds to a Gouy-Chapman length $\lambda = 3$ Å. For such a small value of the Gouy-Chapman length λ, the adsorbed polyampholyte molecules in the Henry (nonoverlapping chain) regime are expected to adopt the "pancake" conformation with thickness $H \sim \lambda_3 = b/f^{1/2}$. For $b = 3$ Å and $f = 1.9 \times 10^{-2}$, the thickness of the adsorbed layer is $H = 22$ Å. The experiments were performed at an ionic strength that corresponds to a Debye length $r_D = 36$ Å. In this range of salt concentrations $r_D > H$, and therefore one can apply the results of the salt-free model to analyze the adsorption isotherms in ref. 131.

The data in ref. 131 clearly indicate that the initial slope of the adsorption isotherms in the gelatin/polystyrene latex system is almost independent of temperature (in the studied range 20–40 °C) and the value of the partition coefficient, that relates the average concentration of polymer in the adsorbed layer to the gelatin concentration, is close to 10. In the framework of the scaling model, the partition coefficient K for an asymmetric polyampholyte in the Henry regime can be estimated as $K = \exp(Nf - \delta fN)$. Using $fN = 22$ (total number of ionized groups in the gelatin molecule), the charge asymmetry $\delta fN = 19$ being estimated from the scaling model for $\lambda = 3$ Å, $r_D = 36$ Å, and $H = 22$ Å, theory predicts $K = \exp(3) = 20$ that is only a factor of two larger than the experimental value $K = 10$.

Detailed experimental verification of the theoretical model of polyampholyte adsorption was also undertaken by Ozon et al.[129] Using atomic force microscopy, they measured the loop size distribution in the adsorbed layers of synthetic polyampholytes at thiol ($HS—(CH_2)_2—SO_3Na$, $HS—(CH_2)_2—CH_3$ and $HS—(CH_2)_2—(CF_2)_7—CF_3$) modified gold surfaces. These experiments correspond to the fence regime in which the average number of monomers in a loop deceases with increasing surface charge density ($g \sim \sigma^{-0.86}$). However, this observed dependence is weaker than that predicted by the scaling theory[97] $g \sim \sigma^{-4/3}$.

Effect of Adsorbed Polyampholytes on Interactions Between Charged Particles

The effect of adsorption of polyampholyte chains on the stability of charged spherical particles was the subject of Monte Carlo simulations by Jonsson et al.[132] These simulations have shown that symmetric polyampholytes reduce the double-layer repulsion between charged spheres, destabilizing the mixtures. The destabilization of the mixture of charged spheres is due to formation of bridges between charged particles comprising adsorbed polyampholytes. This bridging effect is more pronounced for blocky charge sequences, while an alternating charge sequence can only lead to weak attractive interactions. The destabilizing action of adsorbed polyampholytes was traced to chain polarizability.

The force between two charged surfaces in salt-free polyampholyte solution was investigated in the Monte Carlo simulations of Broukhno et al.[124] The authors compare results of three different approximations: (1) polyampholyte chains in the effective mean-field potential of counterions; (2) self-consistent field calculations that take into account the corrections to the distribution of electrostatic potential due to polyampholyte chains; (3) explicit simulation of all interactions. All three methods provide qualitatively similar results. As in the case of charged spheres, the resultant force was found to be strongly dependent on the charge sequence. Thus, for solutions of alternating polyampholytes the effect of polyampholyte chains on the interactions between two charged surfaces is similar to the effect of adding neutral polymers. The authors have argued that alternating polyampholytes have only weak tendency to adsorption at charged surfaces. However, polyampholytes with long blocky charge sequences have been able to displace the electrical double layer of counterions by adsorbing the oppositely charged blocks at the charged surfaces, thereby reducing the surface charge density. At short separations, the adsorbed polyampholytes are able to bridge two surfaces leading to additional attractive interaction. But this attraction can only slightly offset the net repulsive interaction between surfaces and is not sufficient for destabilization.

The interactions between two charged surfaces in solutions of random polyampholytes were calculated by Dobrynin et al.[133] in the framework of the linear response approximation. In the case of symmetric polyampholytes with equal fractions of positively and negatively charged groups, the interaction between charged surfaces is similar to that in electrolyte solutions.[134] In this case, the redistribution of charged monomers at the length scale of the polymer coil leads to effective screening of the surface potential, reducing the electrostatic repulsion between charged surfaces. In the case of charged chains, there is an additional attraction proportional to the charge asymmetry. This result is not surprising, because the asymmetric polyampholytes can be viewed as multivalent macroions. It is well known that even a relatively small amount of multivalent ions substantially screens the surface potential.[134]

Likos et al.[135] have used the combination of DLVO potential and steric potential due to the adsorbed gelatin brush to model the stabilizing forces arising from adsorption of gelatin onto acrylic latex particles of like net charge. Using an integral equation theory for this pair potential, they predicted the small angle neutron scattering from concentrated dispersions of gelatin-coated particles that are in a good quantitative agreement with experimental data.

COMPLEXATION OF POLYAMPHOLYTES WITH POLYELECTROLYTES

Experimental Studies of Polyampholyte–Polyelectrolyte Complexes

Complexes between polyelectrolytes and proteins are well documented in the literature.[136–144] The protein–polyelectrolyte complexes have found applications for protein separation,[138,142,145–147] biosensors development,[148,149] and enzyme immobilization.[150] The interactions of proteins with DNA are central to the control of gene expression and nucleic acid metabolism.[151] The nature

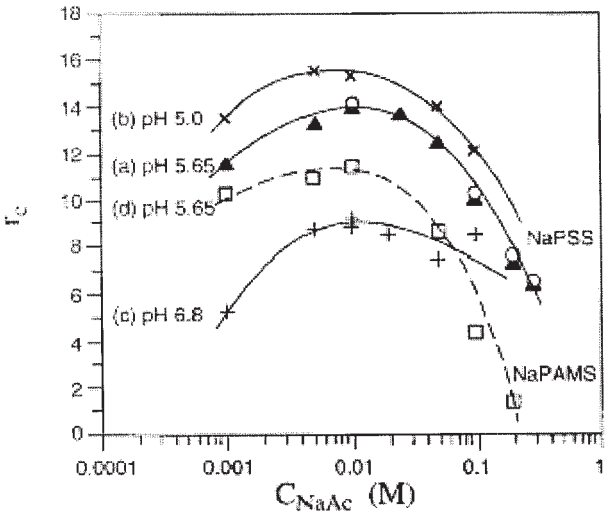

Figure 12. Complex stoichiometry r_c versus salt concentration, at $r = 50$, $T = 40$ °C for gelatin/NaPSS at (a) pH = 5.65 ($M_w = 1.09\ 10^6$) (filled triangles); ($M_w = 5.05\ 10^5$) (open circles); (b) pH = 5.0 ($M_w = 1.09\ 10^6$) (X); (c) pH = 6.8 ($M_w = 1.09\ 10^6$) (+); and for gelatin/NaPAMS ($M_w = 1.1\ 10^6$) at (d) pH = 5.65 (open squares) (from ref. 144).

and generality of soluble protein–polyelectrolyte complexes have been studied extensively using light scattering,[140,144,152–154] electrophoresis,[140,154–159] rheology[160–164] and potentiometric titration.[153,165]

It was established that the binding between polyelectrolytes and proteins occurs in such a way that oppositely charged amino acids on the protein are close to the polyelectrolyte, causing an electrostatic attraction between the two,[166,167] although other factors such as hydrogen bonds, van der Waals interactions, ion release, and water release may also favor complexation in some cases.[167–173] Insoluble complexes are formed when the net charge on the protein is of opposite sign to the charge on the polyelectrolyte. When the protein has a weak net negative charge (above its isoelectric point), it binds to anionic polyelectrolytes to form a complex that remains in aqueous solution.

Gelatin (denatured collagen) exists as a flexible random coil in water above 40 °C. Such coils are easily polarizable in the presence of the polyelectrolyte, putting their oppositely charged amino acids close to the polyelectrolyte backbone. For globular proteins such as albumin and γ-globulins, it is not yet clear whether the proteins denature on binding, assume a different form, or maintain their native form with the polyelectrolyte adapting its conformation to facilitate binding. An important example of complexes with globular proteins is found in synovial fluid, where the anionic polyelectrolyte sodium hyaluronate binds with a variety of proteins.[174–177]

A detailed study of complex formation between negatively charged polyelectrolytes sodium poly(styrene-sulfonate) NaPSS and sodium poly(2-acrylamido-2-methylpropanesulfonate) NaPAMS with gelatin in the range of pH above the isoelectric point of gelatin ($pH_{iso} = 4.9$), where the net charge on the protein is negative, was performed by Bowman et al.[144] Using light scattering, they established that the molecular weight of the single polyelectrolyte chains NaPSS and NaPAMS increase 20- and 15-fold as they complex with gelatin. The gelatin/polyelectrolyte complex has a negative second virial coefficient, indicating a tendency toward interchain complexation as concentration is increased. Indeed, in semidilute solutions reversible gels are formed.[161] The electrostatic nature of the association between polyelectrolytes and gelatin was supported by the effects of pH and salt concentration on the complex stoichiometry r_c, defined as the ratio of the total molecular weight of adsorbed gelatin molecules per polyelectrolyte chain to the molecular weight of the polyelectrolyte chain. The complex stoichiometry decreases monotonically with increasing pH, because this increases the strength of electrostatic repulsion between the polyelectrolyte and gelatin. At constant pH, the complex stoichiometry shows a nonmonotonic dependence on salt concentration (see Fig. 12). The data in Figure 12

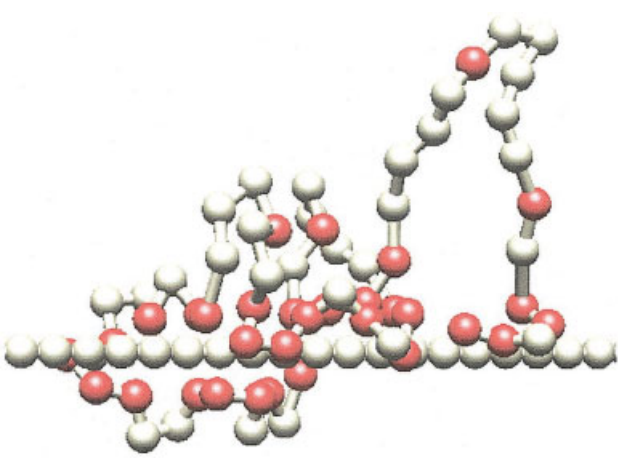

Figure 13. Polarization of a polyampholyte chain near a rod-like anionic polyelectrolyte. Polyelectrolyte monomers and the negatively charged polyampholyte monomers are shown in white, while the positively charged polyampholyte monomers are shown in red.

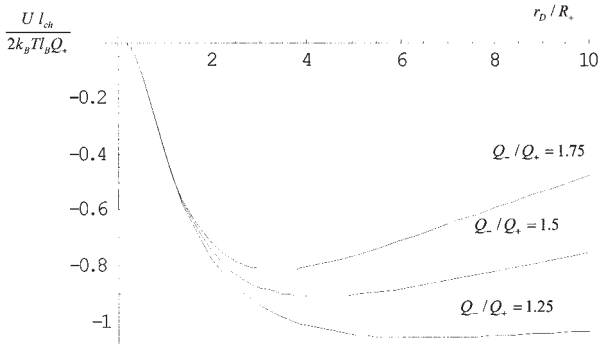

Figure 14. Normalized electrostatic energy of a polyampholyte–polyelectrolyte complex plotted as a function of the reduced Debye radius r_D/R_+ (calculated according to eq 33) at different values of the charge asymmetry Q_-/Q_+ calculated for the ratio of $R_+/R_- = 0.25$.

were measured by light scattering in dilute solutions, with a ratio of gelatin concentration to polyelectrolyte concentration of $r = 50$.

The general trend for the dependence of complex stoichiometry on salt concentration can be understood using the polarization-induced attraction mechanism for complex formation. Near a polyelectrolyte molecule, gelatin molecules are polarized in the electric field created by the polyelectrolyte chain, bringing positively charged groups of gelatin closer to the polyelectrolyte backbone, while displacing negatively charged groups further away (see Fig. 13). The presence of salt leads to an exponential screening of Coulombic interactions. Let the average distance between the positive charges on gelatin eQ_+ and polyelectrolyte backbone be R_+ and the average distance between negative charges on gelatin eQ_- and the polyanion be R_- ($R_+ \leq R_-$). The electrostatic energy between the polarized gelatin and the polyelectrolyte can be estimated as the energy of electrostatic interactions between an asymmetric dipole and a charged rod, with the effective linear charge density l_{ch}^{-1}, where l_{ch} is the average distance between ionized groups on the polyelectrolyte chain. This approximation of assuming a rod-like structure of the polyelectrolyte chain is reasonable at length scales smaller than the Debye screening length r_D where the intrachain electrostatic repulsions between charged groups result in strong chain elongation (see for details ref. 9). The total electrostatic interaction energy is determined by integrating the Yukawa potential over the entire rod.

$$\frac{U_{com}}{k_BT} \approx \frac{l_B}{l_{ch}}\left[-Q_+\int_{-\infty}^{\infty}\frac{\exp(-\sqrt{R_+^2+z^2}/r_D)}{\sqrt{R_+^2+z^2}}\,dz + Q_-\int_{-\infty}^{\infty}\frac{\exp(-\sqrt{R_-^2+z^2}/r_D)}{\sqrt{R_-^2+z^2}}\,dz\right]$$

$$\approx \frac{2l_B}{l_{ch}}(-Q_+K_0(R_+/r_D) + Q_-K_0(R_-/r_D)) \quad (33)$$

The integration in eq 33 is carried out along the polyelectrolyte backbone and $K_0(x)$ is the Bessel function. Figure 14 shows the nonmonotonic dependence of the electrostatic energy of this complex on salt concentration. The initial decrease in the interaction energy is due to the exponential screening of the electrostatic repulsion between the polyanion and the negative charge on gelatin. The subsequent increase in the electrostatic energy of the complex is caused by the screening of the Coulombic attraction—the net charge of the polyelectrolyte chain within the Debye length r_D decreases with increasing salt concentration.

The maximum in protein–polyelectrolyte affinity as a function of salt concentration was also confirmed for globular proteins such as bovine serum albumin, insulin, lysozyme, and beta-lactoglobulin.[178,179] In this case, the protein polarization is associated with alignment of the protein dipole moment in the external electric field of the polyelectrolyte chain. Because globular proteins do not change their conformations upon binding, the position of the maximum net attraction is located at the salt concentration for which the corresponding Debye length is approximately half of the protein diameter, so that the salt screens most of the electrostatic repulsion. It is interesting to note that many physiological conditions have salt concentration of order 0.1 *M*, with Debye length roughly 10 Å, which is comparable to the radius of many globular proteins.

Often, a large contribution to the free energy of binding comes from the counterions released from the polyelectrolyte.[168–171] A single polyampholyte has many positively charged amino acids that can bind to an anionic polyelectrolyte. These positively charged groups partially stabilize the large negative charge that causes counterions to condense on the anionic polyelectrolyte in the absence of polyampholyte. This stabilization allows a bound polyampholyte to release multiple counterions from the polyelectrolyte, making a large portion of the binding free energy entropic in origin.[171]

The soluble polyampholyte–polyelectrolyte complex can behave as a reversible gel (see for review ref. 180) if the concentrations of each species are high enough. This makes the rheological properties of aqueous mixtures of polyampholytes and polyelectrolytes very interesting.[161] The reversible gel nature plays an important role in the utility of such mixtures. A pragmatic example of industrial application of polyampholyte–polyelectrolyte complexes is binding between gelatin and anionic polyelectrolytes. Addition of a small amount of anionic polyelectrolyte boosts the viscosity of gelatin solutions for coating photographic film and paper.[181]

Molecular Simulations of Polyampholyte–Polyelecrolyte Complexes

There are two different classes of molecular simulations of polyelectrolyte–protein complexes. One is in the realm of biochemistry and biophysics where the dominant theme is DNA–protein binding. Here, the main questions are associated with selective recognition of high specificity, essential for protein function, involving high configurational precision. Usually such simulations involve detailed molecular models of DNA, proteins, and solvent and study dynamics of the system on the nanosecond time scale (see for review refs. 182 and 183). The second class is in the domain of polymer science, where polyelectrolyte–polyampholyte systems are represented on the level of coarse-grained chain models that significantly extends accessible time scales by sacrificing details of molecular structure. Here we will review recent results of molecular simulations of coarse-grained models of polyelectrolyte–polyampholyte systems.

Carlsson et al.[184] have performed Monte Carlo simulations of flexible anionic polyelectrolytes with lysozyme. The protein in these simulations was modeled as a charged sphere with a discrete charge distribution corresponding to a projection of the charged residues of the native protein conformation onto the surface of the sphere. The effect of added salt was included in these simulations by modeling electrostatic interactions with a Yukawa (screened Coulomb) potential. The complexation between polyelectrolyte and protein even happened when both species had the same sign of charge, when the protein has a small net charge. For ionic strengths $I = 0.05\ M$ and $0.1\ M$, the onset of complexation occurred when the net charge on the protein was roughly -6. No complexation was observed for strongly negatively charged proteins with net charge <-6. A reentrant complexation transition was found at higher ionic strength ($I = 0.5\ M$). For such high ionic strength, even proteins with a net charge of -13 formed a complex with the negatively charged polyelectrolyte. For all ionic strengths considered in these simulations, the protein polarized by rotating and bound to the middle of the polyelectrolyte chain.

The effects of chain length, ionic strength, and the strength of short-range interactions on protein–polyelectrolyte complexation was studied in Monte Carlo simulations by Carlsson et al.[185] Here, the net protein charge was fixed at $+10$, corresponding to the net charge of lysozyme at pH $= 4.5$. The polyelectrolyte chains in these simulations were negatively charged. At low ionic strengths, the strong electrostatic attraction between protein and polyelectrolyte caused extensive clustering between proteins and polyelectrolytes. As more polyelectrolytes were added to the system a redissolution appeared with proteins forming soluble complexes with polyelectrolytes. Raising salt concentration impeded formation of large clusters by screening the attractive interaction. Increasing the affinity between proteins (strong short-range protein–protein interaction) promotes protein–protein aggregation and facilitates large protein–polyelectrolyte cluster formation.

The effect of charge sequence on complex formation between flexible polyelectrolytes and flexible polyampholytes in dilute salt-free solutions was studied in Monte Carlo simulations by Jeon and Dobrynin.[186] Both polymers were modeled as bead-spring chains of charged Lennard-Jones particles, each consisting of 32 monomers. These simulations have confirmed the polarization origin of complex formation. A polyampholyte chain in a complex is usually located at the *end* of the polyelectrolyte with part of the polyampholyte chain elongated and aligned along the polyelectrolyte backbone. (see Fig. 15) This complex structure between a polarized polyampholyte chain and a polyelectrolyte leads to minimization of the net electrostatic interaction energy. The initially collapsed polyampholytes undergo a globule-coil transition upon forming the complex. Polyampholytes with random charge sequences form stronger complexes with polyelectrolytes than ones with alternating charge sequences but weaker than with blocky polyampholytes. Flexible polyampholytes with a long blocky sequence

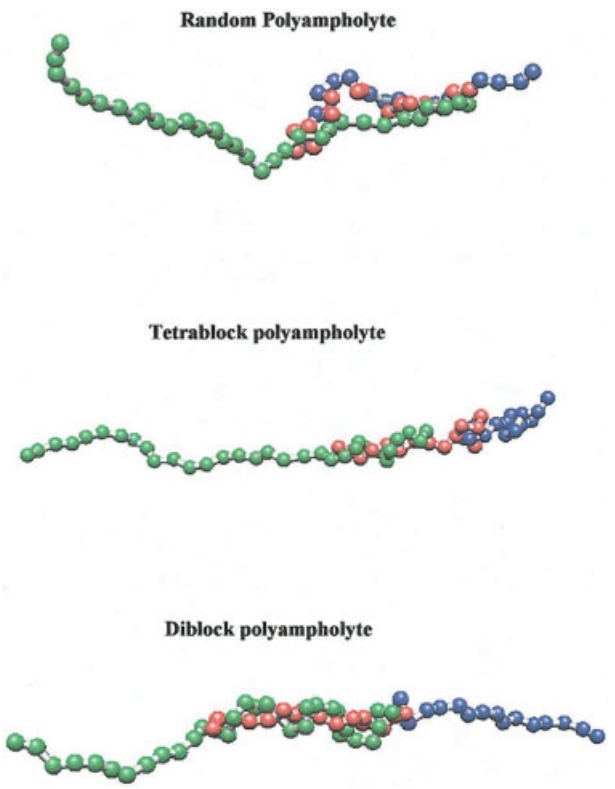

Figure 15. Effect of charge sequence on the structure of polyampholyte–polyelectrolyte complexes. Polyelectrolyte chains are shown in green. Positively charged monomers on polyampholyte chains are shown in red, and negatively charged ones in blue. Snapshots from Monte Carlo simulations by Jeon and Dobyrnin.[186]

form a double helix with the polyelectrolyte at large values of the interaction parameter $u > 4$ (see Fig. 15).

Complexation in a 1 : 1 polyelectrolyte–polyampholyte mixture in dilute and semidilute solutions was the subject of recent molecular dynamics simulations.[187] These simulations have shown that in dilute solutions the chains preferentially form complexes consisting of one polyampholyte chain and one polyelectrolyte chain. As polymer concentration increases, the number of chains in the complexes increases as well. Eventually at polymer concentration $c \sim 0.1\sigma^{-3}$ (where σ is the bead diameter), a fraction of the polyelectrolyte chains and all polyampholytes form one huge micelle. This micelle has an almost neutral core, comprised of sections of both polyelectrolyte and polyampholyte chains. The corona of the micelle consists of sections of polyelectrolyte chains and similarly charged sections of polyampholyte chains (see Fig. 16).

CONCLUSIONS AND OUTLOOK

Conformation of flexible polyampholytes in dilute solutions is controlled by electrostatic interactions between ionized groups. A key to qualitative understanding of fluctuation-induced attraction in polyampholytes is the idea of intrachain Debye length. In salt-free solutions, a polyampholyte chain collapses when its Debye length is smaller than the Gaussian chain size. If there are many Debye volumes per chain volume, each Debye volume is attracted to its neighbor with energy of the order of the thermal energy k_BT. Addition of salt screens this fluctuation-induced attraction when the Debye length due to the salt ions becomes smaller than the Debye length of the polyampholyte chain. Strongly charge-imbalanced polyampholytes behave as polyelectrolytes because electrostatic repulsion between excess charges wins over the fluctuation-induced attraction on larger length scales, forcing the chain to adopt an elongated conformation. The electrostatic repulsion between unbalanced charges is screened by adding salt, thereby lowering the coil size.

The theoretical models of a polyampholyte chain provide a qualitative understanding of the conformations in dilute solutions, but overestimate the strength of the attractive interactions, leading to predicted chain sizes that are smaller than those observed experimentally. It is unclear what causes this discrepancy between theoretical predictions and experiments. One of the possible explanations could be that the dissociation equilibria of the acidic and basic monomers on the chain changes depending on their surrounding environment. As the coil conformation changes, the surrounding environment changes as well and shifts the dissociation equilibrium of the potentially charged monomers.

Charge sequence along the polymer backbone plays an important role in the solution properties of synthetic polyampholytes. Such polymers are produced by random polymerization reactions that lead to a different distribution of the acidic and basic monomers on each chain. Chains can also have different net charge even if the overall composition has equal numbers of positively and negatively charged monomers. A complexation between polyampholytes carrying net opposite charges is one of the reasons for phase separation in polyampholyte solutions.

Contrary to synthetic polyampholytes, the charge sequence of proteins is highly regular. Solutions of proteins contain molecules of similar

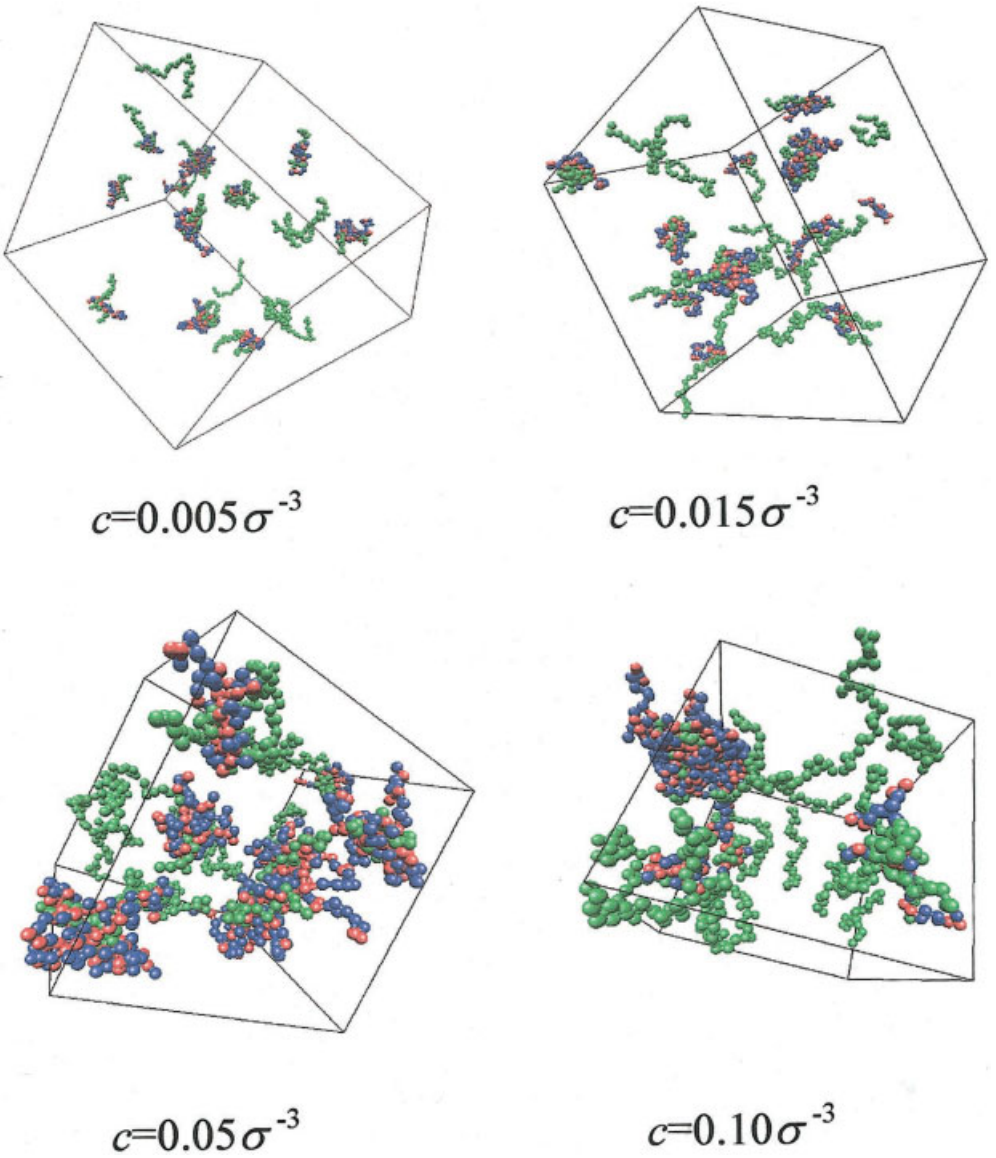

Figure 16. Evolution of polyampholyte–polyelectrolyte aggregates with polymer concentration in a mixture of 20 randomly charged polyampholyte and 20 polyelectrolyte chains of degree of polymerization $N = 32$ and $l_B = 3\sigma$. Polyelectrolyte chains are shown in green. Positively charged monomers on polyampholyte chains are shown in red and negatively charged ones in blue. Snapshots from molecular dynamics simulations by Jeon and Dobrynin.[187]

chemical structure and charge composition. Synthesis of polyampholytes with controlled regular charge sequence has progressed greatly in recent years, but only oligomeric species have been created thus far, owing to the fact that monomers must be added to the chains sequentially. As these synthetic protein analogs are made longer, they will greatly aid our understanding of charge sequence effects on polyampholyte behavior. Quantitative theoretical description of such regular polyampholytes is not yet possible. All theoretical models of polyampholyte chains use preaveraging of the electrostatic interactions over the possible charge sequences. Such a preaveraging approximation significantly simplifies the theoretical calculations of the chain properties, at the expense of the details of the molecular structure. Computer simulations are probably the only practical way to quantify the effect of charge sequence on chain conformations and solution properties.

The interactions of charge-balanced polyampholytes with charged objects of different geometry (polyampholyte adsorption at charged surfaces or their complexation with polyelectrolytes) are due to the polyampholyte chain's polarization in the external electric field created by the charged objects. The polarized chain redistributes its monomers by placing oppositely charged groups closer to the charged object and moving similarly charged groups further away. The polarization-induced attractive interaction is responsible for adsorption of gelatin at charged latex particles and complexation of denatured proteins with polyelectrolytes. The polarization-induced attractive interaction can in some cases lead to effective attraction between charged objects carrying similar net charge. Although there is some understanding of thermodynamics of polyampholyte–polyelectrolyte mixtures, the rheology of protein–polyelectrolyte complexes is still in its infancy. The work in this direction will have far-reaching consequences in the biomedical area. For example, such complexes may control the rheology and lubrication properties of synovial fluid in mammalian joints.

We acknowledge support of the NSF DMR-0305203 (A.V.D.), DMR-0102267 (M.R.), CHE-9876674 (M.R.), ECS-0103307 (M.R.), and of the donors of the Petroleum Research Fund, administered by the American Chemical Society under the grants PRF#37018-AC-7 (M.R.), PRF#39637-AC7 (A.V.D.), and PRF#39287-AC9 (R.H.C.). M.R. also acknowledges financial support of the NASA University Research, Engineering, and Technology Institute on Bio Inspired Materials award NCC-1-02037.

REFERENCES AND NOTES

1. Kudaibergenov, S. E. Adv Polym Sci 1999, 144, 115.
2. Bekturov, E. A.; Kudaibergenov, S. E.; Rafikov, S. R. J Macromol Sci Rev Macromol Chem Phys 1990, C30, 233.
3. Hara, M. Polyelectrolytes; Marcel Dekker: New York, 1993.
4. Mandel, M. In Encyclopedia of Polymer Science and Engineering; Wiley: New York, 1988.
5. Tanford, C. Physical Chemistry of Macromolecules; Wiley: New York, 1961.
6. Schmitz, K. S. Macroions in Solution and Colloidal Suspension; VCH Publishers: Wein, 1993.
7. Oosawa, F. Polyelectrolytes; Marcel Dekker: New York, 1971.
8. Forster, S.; Schmidt, M. Adv Polym Sci 1995, 120, 51.
9. Barrat, J.-L.; Joanny, J.-F. Adv Chem Phys 1996, 94, 1.
10. Radeva, T. Physical Chemistry of Polyelectrolytes; Marcel Dekker: New York, 2001.
11. Alfrey, T., Jr.; Morawetz, H.; Fitzgerald, E. B.; Fuoss, R. M. J Am Chem Soc 1950, 72, 1864.
12. Akabori, S.; Tani, H.; Noguchi, J. Nature 1951, 167, 159.
13. Alfrey, T. Jr.; Morawetz, H. J Am Chem Soc 1952, 74, 436.
14. Alfrey, T., Jr.; Fuoss, R. M.; Morawetz, H.; Pinner, H. J Am Chem Soc 1952, 74, 438.
15. Chiao, Y.-C.; Strauss, U. P. Polym Preprints 1985, 26, 214.
16. Strauss, U. P.; Chiao, Y.-C. Macromolecules 1986, 19, 355.
17. Yang, J. H.; John, M. S. J Polym Sci Part A, Polym Chem 1995, 33, 2613.
18. Zheng, G.-Z.; Meshitsuka, G.; Ishizu, A. J Polym Sci Part B, Polym Phys 1995, 33, 867.
19. Ehrlich, G.; Doty, P. J Am Chem Soc 1954, 76, 3764.
20. Katchalsky, A.; Miller, I. R. J Polym Sci 1954, 13, 57.
21. McCormick, C. L.; Salazar, L. C. Macromolecules 1992, 25, 1896.
22. Salamone, J. C.; Amhed, I.; Rodriguez, E. L.; Quach, L.; Watterson, A. C. J Macromol Sci 1988, A25, 811.
23. Salamone, J. C.; Quach, L.; Watterson, A. C.; Krauser, S.; Mahmud, M. U. J Macromol Sci 1985, A22, 653.
24. Johnson, C. B.; McCormick, C. L. Polym Mater Sci Eng 1987, 57, 154.
25. McCormick, C. L.; Johnson, C. B. Macromolecules 1988, 21, 694.
26. Salamone, J. C.; Amhed, I.; Raheja, M. K.; Elayaperumal, P.; Watterson, A. C.; Olson, A. P. In Water-Soluble Polymers for Petroleum Recovery; Stahl, G. A., Schulz, D. N., Eds.; Plenum: New York, 1988; p 181.
27. McCormick, C. L.; Salazar, L. C. J Appl Polym Sci 1993, 48, 1115.
28. Corpart, J.-M.; Candau, F. Macromolecules 1993, 26, 1333.
29. Wagner, H. L.; Long, F. A. J Phys Coll Chem 1951, 55, 1512.
30. Morawetz, H. Macromolecules in Solution; Wiley: New York, 1975.
31. Baker, J. P.; Stephens, D. R.; Blanch, H. W.; Prausnitz, J. M. Macromolecules 1992, 25, 1955.
32. Baker, J. P.; Blanch, H. W.; Prausnitz, J. M. Polymer 1995, 36, 1061.
33. Katchalsky, A.; Shavit, N.; Eisenberg, H. J Polym Sci 1954, 13, 69.

34. Katchalsky, A.; Gillis, J. Recl Trav Chim Pays-Bas 1949, 68, 879.
35. Mazur, J.; Silberberg, A.; Katchalsky, A. J Polym Sci 1959, 35, 43.
36. Salamone, J. C.; Tsai, C. C.; Olson, A. P.; Watterson, A. C. In Ions in Polymers; Eisenberg, A., Ed. American Chemical Society: Washington, DC, 1980; p 337.
37. Salamone, J. C.; Tsai, C. C.; Olson, A. P.; Watterson, A. C. Polym Preprints 1978, 19, 261.
38. Guo, L.; Colby, R. H.; Lusignan, C. P.; Howe, A. M. Macromolecules 2003, 36, 10009.
39. McCormick, C. L.; Johnson, C. B. Polymer 1990, 31, 1100.
40. McCormick, C. L.; Johnson, C. B. Macromolecules 1988, 21, 686.
41. McCormick, C. L.; Johnson, C. B. J Macromol Sci 1990, A27, 539.
42. McCormick, C. L.; Salazar, L. C. Polymer 1992, 33, 4384.
43. McCormick, C. L.; Salazar, L. C. J Macromol Sci 1992, A29, 193.
44. Wielema, T. A.; Engberts, J. B. F. N. Eur Polym J 1990, 26, 639.
45. Lee, W.-F.; Chen, C.-F. Polym.Gels Networks 1998, 6, 493.
46. English, A. E.; Mafe, S.; Manzanares, J. A.; Yu, X.; Grosberg, A. Y.; Tanaka, T. J Chem Phys 1996, 104, 8713.
47. Peiffer, D. G.; Lundberg, R. D. Polymer 1985, 26, 1058.
48. Skouri, M.; Munch, J. P.; Candau, S. J.; Neyret, S.; Candau, F. Macromolecules 1994, 27, 69.
49. Ohlemacher, A.; Candau, F.; Munch, J. P.; Candau, S. J. J Polym Sci Part B, Polym Phys 1996, 34, 2747.
50. Candau, F.; Ohlemacher, A.; Munch, J. P.; Candau, S. J. Rev Instit Francais Petrole 1997, 52, 133.
51. Lowe, A. B.; McCormick, C. L. Chem Rev 2002, 102, 4177.
52. Hart, R.; Timmerman, D. J Polym Sci 1958, 28, 638.
53. Salamone, J. C.; Volksen, W.; Olson, A. P.; Israel, S. C. Polymer 1978, 19, 1157.
54. Wielema, T. A.; Engberts, J. B. F. N. Eur Polym J 1990, 26, 415.
55. Lee, W.-F.; Chen, Y.-M. J Appl Polym Sci 2003, 89, 1884.
56. Schulz, D. N.; Peiffer, D. G.; Agarwal, P. K.; Larabee, J.; Kaladas, J. J.; Soni, L.; Handwerker, B.; Garner, R. T. Polymer 1986, 27, 1734.
57. Muroga, Y.; Amano, M.; Katagiri, A.; Noda, I.; Nakaya, T. Polym J 1995, 27, 65.
58. Kato, T.; Takahashi, A. Ber Bunsenges Phys Chem 1996, 100, 784.
59. Ali, S. A.; Rasheed, A. Polymer 1999, 40, 6849.
60. Berlinova, I. V.; Dimitrov, I. V.; Kalinova, R. G.; Vladimirov, N. G. Polymer 2000, 41, 831.
61. Liaw, D.-J.; Huang, C.-C.; Sang, H.-C.; Wu, P.-L. Polymer 2000, 41, 6123.
62. Liaw, D.-J.; Huang, C.-C.; Sang, H.-C.; Kang, E.-T. Polymer 2001, 42, 209.
63. Niu, A.; Liaw, D.-J.; Sang, H.-C.; Wu, C. Macromolecules 2000, 33, 3492.
64. Xue, W.; Huglin, M. B.; Khoshdel, E. Polym Int 1999, 48, 8.
65. Viklund, C.; Irgum, K. Macromolecules 2000, 33, 2539.
66. Viklund, C.; Sjogren, A.; Irgum, K. Anal Chem 2001, 73, 444.
67. Edwards, S. F.; King, P. R.; Pincus, P. Ferroelectrics 1980, 30, 3.
68. McQuarrie, D. A. Statistical Mechanics; Harper: New York, 1976.
69. Dobrynin, A. V.; Rubinstein, M. J Phys II 1995, 5, 677.
70. Bratko, D.; Chakraborty, A. K. J Phys Chem 1996, 100, 1164.
71. Higgs, P. G.; Joanny, J.-F. J Chem Phys 1991, 94, 1543.
72. Rubinstein, M.; Colby, R. H. Polymer Physics; Oxford University Press: London, 2003.
73. Grosberg, A. Y.; Khokhlov, A. R. Statistical Physics of Macromolecules; AIP Press: New York, 1994.
74. Yamakov, V.; Milchev, A.; Limbach, H. J.; Dunweg, B.; Everaers, R. Phys Rev Lett 2000, 85, 4305.
75. Kantor, Y.; Li, H.; Kardar, M. Phys Rev Lett 1992, 69, 61.
76. Kantor, Y.; Kardar, M.; Li, H. Phys Rev E 1994, 49, 1383.
77. Kantor, Y.; Kardar, M. Europhys Lett 1994, 27, 643.
78. Kantor, Y.; Kardar, M. Phys Rev E 1995, 51, 1299.
79. Kantor, Y.; Kardar, M. Phys Rev E 1995, 52, 835.
80. Srivastava, D.; Muthukumar, M. Macromolecules 1996, 29, 2324.
81. Tanaka, M.; Grosberg, A. Yu.; Pande, V. S.; Tanaka, T. Phys Rev E 1997, 56, 5798.
82. Soddemann, T.; Schiessel, H.; Blumen, A. Phys Rev E 1998, 57, 2081.
83. Victor, J. M.; Imbert, J. B. Europhys Lett 1993, 24, 189.
84. Wang, Z.; Shusharina, N.; Rubinstein, M. Macromolecules 2004, in press.
85. Wittmer, J.; Johner, A.; Joanny, J. F. Europhys Lett 1993, 24, 263.
86. Pande, V. S.; Grosberg, A. Yu.; Joerg, C.; Kardar, M.; Tanaka, T. Phys Rev Lett 1996, 77, 3565.
87. Angerman, H. J.; Shakhnovich, E. I. J Chem Phys 1999, 111, 772.
88. Pande, V. S.; Grosberg, A. Y.; Tanaka, T. Rev Modern Phys 2000, 72, 259.

89. Gutin, A. M.; Shakhnovich, E. I. Phys Rev E 1994, 50, R3322.
90. Dobrynin, A. V.; Rubinstein, M.; Obukhov, S. P. Macromolecules 1996, 29, 2974.
91. Solis, F. J.; Olvera de La Cruz, M. Macromolecules 1998, 31, 5502.
92. Lyulin, A. V.; Dunweg, B.; Borisov, O. V.; Darinskii, A. A. Macromolecules 1999, 32, 3264.
93. Chodanowski, P.; Stoll, S. J Chem Phys 1999, 111, 6069.
94. Micka, U.; Holm, C.; Kremer, K. Langmuir 1999, 15, 4033.
95. Micka, U.; Kremer, K. Europhys Lett 2000, 49, 189.
96. Lee, N.; Obukhov, S. Eur Phys J B 1999, 1, 371.
97. Dobrynin, A. V.; Rubinstein, M.; Joanny, J. F. Macromolecules 1997, 30, 4332.
98. Tanaka, M.; Grosberg, A. Y.; Tanaka, T. Langmuir 1999, 15, 4052.
99. Tanaka, M.; Grosberg, A. Y.; Tanaka, T. J Chem Phys 1999, 110, 8176.
100. Everaers, R.; Johner, A.; Joanny, J. F. Europhys Lett 1997, 37, 275.
101. Everaers, R.; Johner, A.; Joanny, J. F. Macromolecules 1997, 30, 8478.
102. Tanaka, M.; Tanaka, T. Phys Rev E 2000, 62, 3803.
103. Gonzalez-Mozuelos, P.; Olvera de La Cruz, M. J Chem Phys 1994, 100, 507.
104. Dobrynin, A. V. J Phys II 1995, 5, 1241.
105. Schiessel, H.; Oshanin, G.; Blumen, A. J Chem Phys 1995, 103, 5070.
106. Schiessel, H.; Blumen, A. J Chem Phys 1996, 104, 6036.
107. Schiessel, H.; Blumen, A. J Chem Phys 1996, 105, 4250.
108. Winkler, R. G.; Reineker, P. J Chem Phys 1997, 106, 2841.
109. Schiessel, H.; Blumen, A. Macromol Theory Simulat 1997, 6, 103.
110. Chen, Y.; Shew, C. Y. Chem Phys Lett 2003, 378, 142.
111. Ward, A. G.; Courts, A. The Science and Technology of Gelatin; Academic Press: London, 1977.
112. Cox, R. J. Photographic Gelatin; Academic Press: London, 1972.
113. Curme, H. G.; Natale, C. C. J Phys Chem 1964, 68, 3009.
114. Berendsen, R.; Borginon, H. J Photograph Sci 1968, 16, 194.
115. Kragh, A. M.; Peacock, R. J Photograph Sci 1967, 15, 220.
116. Kawanishi, N.; Christenson, H. K.; Ninham, B. W. J Phys Chem 1990, 94, 4611.
117. Kamiyama, Y.; Israelachvili, J. Macromolecules 1992, 25, 5081.
118. Neyret, S.; Ouali, L.; Candau, F.; Pefferkorn, E. J Colloid Interface Sci 1995, 187, 86.
119. Netz, R. R.; Joanny, J.-F. Macromolecules 1998, 31, 5123.
120. Dobrynin, A. V.; Obukhov, S. P.; Rubinstein, M. Macromolecules 1999, 32, 5689.
121. Zhulina, E. B.; Dobrynin, A. V.; Rubinstein, M. Eur Phys J E 2001, 5, 41.
122. Dobrynin, A. V.; Zhulina, E. B.; Rubinstein, M. Macromolecules 2001, 34, 627.
123. Zhulina, E.; Dobrynin, A. V.; Rubinstein, M. J Phys Chem B 2001, 105, 8917.
124. Broukhno, A.; Khan, M. O.; Akesson, T.; Jonsson, B. Langmuir 2002, 18, 6429.
125. Khan, M. O.; Akesson, T.; Jonsson, B. J Chem Phys 2002, 116, 3917.
126. Joanny, J.-F. J Phys II 1994, 4, 1281.
127. Bermel, P.; Dobrynin, A. V.; Rubinstein, M. (unpublished) 2001.
128. Khan, M. O.; Akesson, T.; Jonsson, B. Macromolecules 2001, 34, 4216.
129. Ozon, F.; di Meglio, J.-M.; Joanny, J.-F. Eur Phys J E 2002, 8, 321.
130. Hone, J. H. E.; Howe, A. M.; Whitesides, T. H. Colloids Surfaces A, Physicochem Eng Aspects 2000, 162, 283.
131. Vaynberg, A. K.; Wagner, N. J.; Sharma, R.; Martic, P. J Colloid Interface Sci 1998, 205, 131.
132. Jonsson, B.; Khan, M. O.; Akesson, T.; Woodward, C. E. Langmuir 2002, 18, 1426.
133. Dobrynin, A. V.; Rubinstein, M.; Joanny, J.-F. J Chem Phys 1998, 109, 9172.
134. Israelachvili, J. Intermolecular and Surface Forces; Academic Press: London, 1992.
135. Likos, C. N.; Vaynberg, A. K.; Lowen, H.; Wagner, N. J. Langmuir 2000, 16, 4100.
136. Dubin, P. L.; Farinato, R. S. Colloid–Polymer Interactions: From Fundamentals to Practice; Wiley-Interscience: New York, 1999.
137. Kokufuta, E. In Macromolecular Complexes in Chemistry and Biology; Dubin, P., Bock, J., Davis, R., Schluz, D. N., Thies, C., Eds.; Springer-Verlag: Berlin, 1994; p 301.
138. Niederauer, M. Q.; Glatz, C. E. Adv Biochem Eng 1992, 47, 159.
139. Park, J. M.; Muhoberac, B. B.; Dubin, P. L.; Xia, J. Macromolecules 1992, 25, 290.
140. Xia, J.; Dubin, P. L.; Kim, Y.; Muhoberac, B. B.; Klinkowski, V. J. J Phys Chem 1993, 97, 4528.
141. Ahmed, L. S.; Xia, J.; Dubin, P. L.; Kokufuta, E. J Macromol Sci, Pure Appl Chem 1994, A31, 17.
142. Dubin, P.; Bock, J.; Davies, R.; Schluz, D. N.; Thies, C. Macromolecular Complexes in Chemistry and Biology; Springer-Verlag: Berlin, 1994.
143. Izumrudov, V. A. Berichte der Bunsen-Gesellschaft [Phys Chem Chem Phys] 1996, 100, 1017.
144. Bowman, W. A.; Rubinstein, M.; Tan, J. S. Macromolecules 1997, 30, 3262.
145. Dubin, P.; Gao, J.; Mattison, K. Sep Purif Methods 1994, 23, 1.

146. Jiang, J.; Prausnitz, J. M. J Phys Chem B 1999, 103, 5560.
147. Jiang, J.; Prausnitz, J. M. J Phys Chem B 2000, 104, 7197.
148. Muller, M.; Brissova, M.; Rieser, T.; Powers, A. C.; Lunkwitz, K. Mater Sci Eng 1999, C8–9, 163.
149. Griffith, A.; Glidle, A.; Cooper, J. M. Biosensors Bioelectron 1996, 11, 625.
150. Kokufuta, E. Prog Polym Sci 1992, 17, 647.
151. Mathews, C. K.; Van Holde, K. E.; Ahern, K. G. Biochemistry; Benjamin/Cummings: San Francisco, 2000.
152. Li, Y.; Mattison, K. W.; Dubin, P. L.; Havel, H. A.; Edwards, S. L. Biopolymers 1996, 38, 527.
153. Mattison, K. W.; Dubin, P. L.; Brittain, I. J. J Phys Chem B 1998, 102, 3830.
154. Gao, J. Y.; Dubin, P. L.; Muhoberac, B. B. J Phys Chem B 1998, 102, 5529.
155. Gao, J. Y.; Dubin, P. L.; Muhoberac, B. B. Anal Chem 1997, 69, 2945.
156. Hallberg, R. K.; Dubin, P. L. J Phys Chem B 1998, 102, 8629.
157. Xia, J.; Dubin, P. L.; Kokufuta, E.; Havel, H.; Muhoberac, B. B. Biopolymers 1999, 50, 153.
158. Porcar, I.; Gareil, P.; Tribet, C. J Phys Chem 1998, 102, 7906.
159. Porcar, I.; Cottet, H.; Gareil, P.; Tribet, C. Macromolecules 1999, 32, 3922.
160. Tribet, C.; Porcar, I.; Bonnefont, P. A.; Audebert, R. J Phys Chem B 1998, 102, 1327.
161. Colby, R. H. 2000. Proceedings of the XIIIth International Congress on Rheology, 1–414.
162. Petit, F.; Audebert, R.; Iliopoulos, I. Colloid Polym Sci 1995, 273, 777.
163. Borrega, R.; Tribet, C.; Audebert, R. Macromolecules 1999, 32, 7798.
164. Tribet, C. In Physical Chemistry of Polyelectrolytes; Radeva, T., Ed.; Marcel Dekker: New York, 2001.
165. Wen, Y.-P.; Dubin, P. L. Macromolecules 1997, 30, 7856.
166. Marky, N. L.; Manning, G. S. J Am Chem Soc 2000, 122, 6057.
167. Jayaram, B.; McConnell, K.; Dixit, S. B.; Das, A.; Beveridge, D. L. J Comput Chem 2002, 23, 1.
168. Record, M. T.; Lohman, T. M.; de Haseth, P. J Mol Biol 1976, 107, 145.
169. Record, M. T.; Anderson, C. F.; Lohman, T. M. Q Rev Biophys II 1978, 2, 103.
170. Mascotti, D. P.; Lohman, T. M. Proc Natl Acad Sci USA 1990, 87, 3142.
171. Jayaram, B.; DiCapua, F. M.; Beveridge, D. L. J Am Chem Soc 1991, 113, 5211.
172. Luscombe, N. M.; Laskowski, R. A.; Thornton, J. M. Nucleic Acids Res 2001, 29, 2860.
173. Reddy, C. K.; Das, A.; Jayaram, B. J Mol Biol 2001, 314, 619.
174. Swann, D. A.; Caulfield, J. B.; Ceselski, A. Ann Rheum Dis 1975, 34(Suppl), 98.
175. Swann, D. A.; Caulfield, J. B. Conn Tissue Res 1975, 4, 31.
176. Swann, D. A. In The Joints and Synovial Fluid; Sokoloff, L., Ed. Academic Press: New York, 1978; p 407.
177. Krause, W. E. 2000. Solution Dynamics of Synthetic and Natural Polyelectrolytes. Doctoral Dissertation, Pennsylvania State University.
178. Seyrek, E.; Dubin, P. L.; Tribet, C.; Gamble, E. A. Biomacromolecules 2003, 4, 273.
179. Hattori, T.; Hallberg, R.; Dubin, P. L. Langmuir 2000, 16, 9738.
180. Rubinstein, M.; Dobrynin, A. V. Curr Opin Colloid Interface Sci 1999, 4, 83.
181. Uhrich, C.; Nawn, G. Photo Sci Eng 1970, 14, 178.
182. Giudice, E.; Lavery, R. Acc Chem Res 2002, 35, 350.
183. Cheatham, T. E. III; Young, M. A. Biopolymers (Nucleic Acid Sci) 2001, 56, 232.
184. Carlsson, F.; Linse, P.; Malmsten, M. J Phys Chem B 2001, 105, 9040.
185. Carlsson, F.; Malmsten, M.; Linse, P. J Am Chem Soc 2003, 125, 3140.
186. Jeon, J.; Dobrynin, A. V. Phys Rev E 2003, 67, 0618031.
187. Jeon, J.; Dobrynin, A. V. Macromolecules 2004, to be published.